

We would like to thank the reviewers for their comments. Since some of the comments required rather large changes to the code, the model description in the revised manuscript has changed significantly. We have merged the model with other parts of the ORCHIDEE-CAN version, which is described in Naudts et al. (2015).

We have implemented a new method to calculate the albedo of a canopy based on the vertical vegetation profile (McGrath et al., in prep.). The vertical profile of the albedo allows us to calculate more accurately the vertical distribution of short wave radiation, which for canopy models, affects directly the calculation of the energy budget at each level, hence the leaf temperature, and consequently the resulting sensible and latent heat fluxes.

We have introduced an improved calculation of stomatal conductance. The multi-layer model as described in the previous version of the article applied the light-dependent formulation of Lohanner et al. (1980), after Jarvis (1976). It was originally intended as a means to evaluate the balance and stability of the model before the implementation of a more complete scheme. We have now replaced this with the scheme of Ball et al. (1987). The implementation of these changes have resulted in a delay in the production of a revised manuscript. Line references here refer to the ‘track changes’ document.

Anonymous Referee #1

Received and published: 16 January 2015

General

The paper presents (1) a new multilayer scheme to treat vegetation and soil within the ORCHIDEE model and (2) an algorithm to apply the so-called implicit backward method for solving the prognostic equations. This method permits simulations with a much longer time step than the more common explicit method, but requires the efficient solution of a system of coupled equations (many equations if a multilayer scheme is used), a problem that is solved in the Supplement. It also presents a first attempt to validate the model with observations, in which versions with various numbers of layers are also compared. As the authors indicate, the first two points contain not very novel ideas, but thus far they have rarely been used in combination in soil-vegetation-atmosphere modelling, because of the numerical complications involved. It is therefore courageous of the authors to implement these relatively old, but valid existing developments in current land surface modelling schemes.

Concerning the first point: the description is often all too elaborate for what concerns generally known processes (balance equations etc.). On the other hand, information about specific points and the accompanying references (parameterization of resistances and radiation) is sometimes incomplete. We also found some issues with signs in equations, and with the interpretation of resistances in the model, which need to be cleared (see minor points). These issues also

occur in the accompanying paper of Naudts et al.

By design soil-vegetation-atmosphere models bring together three research communities; i.e., soil, vegetation and atmospheric science. The lengthy explanation of the balance equations was a deliberate choice in order to explain the design of the model to readers from the soil and vegetation community who may not have a background in the Physical Sciences. On the other hand, we have relied on references for many of the details of the parameterisations. We retain the former for the reasons given, but we have followed this recommendation and therefore the revised manuscript provides more details with regard to the latter (Section 3.2). We have also corrected the signs problems founds in the equations.

A more general question: how is the wetting of the vegetation and soil by rain taken into account? It does not occur in the core equations.

Both soil interactions and leaf level evaporation components are parameterised using the same interception and evaporation coefficients as are used in the existing ORCHIDEE model (Krinner et al, 2005; IPSL/LSCE, 2012), of which ORCHIDEE-CAN is an extension. A portion of rainfall is intercepted by the vegetation, as determined by the total canopy LAI, where it will be subject to evaporation as standing water. The rest falls on the soil surface, and is treated in the same way as for bare soil in the existing model. We added this explanation as Section 3.3.

Concerning the second point: the simplest implicit approach, based on the backward time difference, is used (this could be indicated explicitly in the paper, as there are other implicit methods available). Such an approach is not uncommon for problems with one unknown per layer (vertical diffusion of heat and constituents in the atmosphere), but here it is applied to three unknowns per layer. The problem is then solved by two ‘sweeps’ in opposite direction, as suggested by Richtmyer and Morton (1967). This approach is entirely valid, but we would like a confirmation of the authors that the results have been checked for exact agreement with all the original balance equations (without sign errors etc.), including the boundary conditions, to remove any doubt.

The model operations have been checked so that all components that are driven by the new scheme balance exactly at the top of canopy. This means that the following equation is satisfied:

$$(LW_{\downarrow}+SW_{\downarrow}) = (LW_{\uparrow}+SW_{\uparrow})+(H+\lambda E)+\Delta(C_p^{air}T_a)+\Delta(q_a)+\Delta(C_p^{veg}T_L)+J_{soil}+\theta_0\Delta T_{surf} \quad (1)$$

The boundary conditions are outlined in the supplementary material. The upper boundary condition is set either by contents of the forcing file or from the coefficients that are passed to the canopy model by the atmospheric transport model LMDz. The lower boundary condition includes the term J_{soil} , which is

the soil flux derived from the existing sub-soil energy scheme within the ORCHIDEE trunk (De Rosnay, 1999; De Rosnay et al., 2003; d’Orgeval et al., 2008). While implementing, debugging and testing the code, energy budget closure was checked at every layer for every time step. Such sign errors had already been detected and accounted for in the code, though remained in the first submitted version of the manuscript.

The explanation in the Supplement is very long and, for the details of the implicit method, very hard to follow. Below we suggest a thorough condensation of the description, which could be made with little work, and which would be of more help to interested readers. On comparing the induction methods in the supplement with the methods of Richtmyer and Morton (RM) to which the authors refer, we note that the authors have chosen a method which is essentially different and more involved than RM’s, and requires quite a long-winded derivation. This is not required since, as far as we can see, the problem can be translated with little effort so as to match RM’s framework. By doing so, it appears that hardly any further derivation is necessary. Below we add an explanatory note (‘An easy alternative for the induction’), which we suggest to be discussed in the reply.

We would like to thank the reviewer for the effort that they have made to review the derivation itself. While working on the derivation we did not use the RM approach, which nevertheless appears valid to us. However, it does assume familiarity with the references noted, and we think that the outline of derivations provided here is useful for the non-specialist to better understand the structure of the model. We propose a consensus solution in which we keep our initial derivation as it best matches the source code and for which the supplementary material acted as a coding template and subsequently as documentation. We added the derivation suggested by the reviewers in the supplementary material (section S 3.15) as an alternative derivation and refer to it in the manuscript (section 3.5.6, line 422), that can be referred to by those with a background in numerical methods. As the reviewers note, the two methods produce the same results.

Concerning the third point (validation): The paper offers evidence for the wider possibilities of a multilayer approach compared to a one-layer approach. Getting the details correct is a difficult pioneering work, however, as information on the proper parameterisation of separate layers and of K is scarce and difficult to judge.

We have made an effort to better document the parameterization of the separate layers and K (Section 4.3, and Table 3) but decided to leave out a comprehensive description because this would result in an even longer manuscript. Nevertheless, a parameterization for different temperate and boreal forests is the topic for a follow-up paper currently in the final stages of preparation (Chen et al), for which a total of eight test sites for which detailed in-canopy measurements

have been made available for a detailed evaluation of the model. Within the limitations of the model compared to a more iterative and detailed scheme, we demonstrate with the Tumbarumba site that a good simulation is possible using only a small number of parameterisation factors.

Minor comments (paper)

Passim: Notation: use curly d and not delta for partial differentiation. Further, if you assume that a variable like q_{sat} depends on one parameter (T), the derivative should just be written using 'd'.

Corrected (eqns. 16-20; eqns. 25-30)

8651, Eq. 1: H and LE require a minus sign, according to the convention given in the first sentence of the results section and elsewhere.

This sign error has been corrected in the manuscript. (eqn. 1 and following).

8655, lines 8-9: It would seem that instabilities in an atmospheric model are better remedied within that model...

Corrected to: 'if there is an instability in the land surface model, it will tend to be dampened in subsequent timesteps' (Line 133)

8656, line 2: Table 1 is not complete, it does not contain parameters which occur only locally in the text, this might be indicated in the reference to the table.

We have now included all symbols which occur throughout the text in Table 1.

8656, line 15: 'stimulate' delete 't'.

Corrected (Line 160)

8656, line 22: important R_i ? is introduces as the stomatal resistance but in the subsequent equations, R_i ? makes only sense as the sum of stomatal and aerodynamic resistance. There is a similar problem with the companion discussion paper by Naudts et al. (page 8590 etc.) where R_a also has a wrong description.

R_i ? does refer to the sum of stomatal and aerodynamic resistances, and so this has been clarified (section 3.2). As also requested by another reviewer, more detail on the calculation of aerodynamic resistance has been provided (section 3.2).

8658: are L and lambda the same? the paper and the supplement should use a consistent notation.

Yes, both correspond to the Latent Heat of Vaporisation - L is now expressed as lambda throughout (e.g. Eqn. 1).

8658, eq. 8: explain R (gas constant per kg ?).

R is the molar gas constant $R = 8.314 \text{ J mol}^{-1} \text{ K}^{-1}$? no longer appears as this section abridged in accordance to comment regarding the leaf vapour pressure assumption, below.

8658: The derivations are a bit lengthy; the final form contains approximations which might have been introduced earlier. Moreover, less explicit explanation would do as this is common textbook knowledge.

The humidity-saturation curve is textbook knowledge for Physicists but is included for ease of reference to readers from other backgrounds. As a land surface model, many readers might be from an interdisciplinary background, such as geography, biology or soil science. The explanation had been shortened, however (section. 3.1 and throughout supplementary material).

8659: Section 3.2: The explanations should be more explicit.

This section has been expanded to include fuller details of the derivation of R_i and an updated parameterisation of R_i (section 3.2)

8659, line 16: θ should be termed specific heat not heat capacity. And use a little θ , the big Θ has a different meaning.

Description changed to 'specific heat'. Symbols updated so that we now have θ_i^{leaf} for vegetation layer specific heat capacity, and C_p^a for specific heat (Eq 15, 23 and throughout supplementary material).

8659, Eq. 12: not sure about the signs of H and LE.

We updated the sign convention to reflect positive flux as that which leaves vegetation, negative flux entering (as is already the case for the soil surface), so the signs for H and LE are changed to negative (Eq 15, 24, 30 and throughout supplementary material)

8660, line 4: the reference to Eq. 8 should apparently be to Eq. 12.

Corrected (section 3.4, now to eq. 14)

8660: Eq. 13: here the signs are certainly wrong ! Also in the supplement, S2.14 and later. The same error occurs in Eq. 35 in the companion discussion paper by Naudts et al.

Corrected (section 3.5.3), also corrected in corresponding equation of Naudts et al. during typesetting stage

8660, eq. 13: Explain Θ .

This is the heat capacity of air, but it is renamed as C_p^{air} in the text (from Θ). (Eq 23)

8660, eq. 14: First term in the right hand side: what is Γ ?. The second term is explained as a 'concentration' whereas one would expect 'source density' (8661 line 13).

Γ is the concentration to gradient relationship across any dimension, restricted to the z-axis, as $k(z)$, in the equation that follows. A more detailed explanation has been added. 'Source density' is a more precise term than 'concentration', so the description has been updated.

8660: lines 4-8 should be rewritten.

The terms 'resistance to sensible heat flux' and 'resistance to latent heat flux' have been replaced, respectively, with 'combined leaf to atmosphere temperature resistance' and 'combined leaf to atmosphere specific humidity resistances'. (Line 296)

8661: Eq. 15: This form is incorrect (unless k is independent of z) and superfluous.

This line removed, as k is indeed dependent on z . (Eq 17)

8661: Eq. 17 has a wrong sign (see Eq. 18).

Corrected (Eq 18)

8661: line after Eq. 17 : is x ever used ? If not this should be deleted.

We start in general terms for the reader unfamiliar with the technique. This method can be applied in other canopy transport scenarios, for example for gas species or aerosol transport, so χ (not x) should stay to make this point, that it is not just the state variables of T and q to which this equation can be applied.

8662: the notation 'R' introduced here, has already been used for resistances and for the gas constant. Maybe a subscript should be added for better discernment.

Further, it should not be called 'correction term' but 'correction factor' (line 8).

We add a subscript for R_{NF} (for near field). We replace 'correction term' with 'correction factor', as suggested (Line 338).

8662: the explanation of 'k' is not very intelligible; no clues about the calculation of w ; the definition of TL (symbol was earlier used for leaf temperature!) and τ is rather esoteric. How does the leaf area density enter in the calculations? It seems it is only mentioned in the discussion (8677 line 3).

This is direct from the derivation of Raupach (1989a), and broadly applied across the field since. The implementation of the leaf area density in the calculation is described in the referenced second order closure model of Massman & Weil (1999), and we use here the same symbols as in those works. The derivation of both expressions is rather too lengthy for inclusion here, but a fuller explanation of the origin has been added (Line 327-333) such that the reader does not need to consult the original studies to understand the set-up of our multi-layer model. The symbol TL in the manuscript has been changed to 'Tleaf' where it refers to leaf temperature and remains as TL to denote the Lagrangian timescale.

8663, Eq. 22: ΔA should be ΔV ; also in Eq. 26 etc.

Corrected (eq. 23, eqs. 27-29)

8663, Eq. 24 and also Eq. 28 on the next page, contain a wrong expression with second order derivative (wrong because k depends on z). Such expressions are moreover not used, one uses the difference between the fluxes at the top and bottom of the layer.

These expressions (now 25 and 29) have been revised with the k coefficient moved inside the derivative. The subsequent, differenced, expressions (33 and 34) were already correct.

8664: line 7: 'vegetation level' should be 'canopy air level' ?

Corrected (Line 378)

8664, line 8: 'atmosphere' better is to use here 'air'.

Updated as suggested (Line 380)

8665: Eq. 31: Explain η so that the reader has not to look it up in the supplement.

A fuller description of long-wave radiation scheme has been added here (section 3.7).

8666: Eqs. 32-33 have superfluous brackets.

Some brackets removed (Eqs. 33, 34)

8666: Eq. 39: '-Jsoil' belongs within the brackets.

Corrected (Eq 40)

8666, line 9: Reformulate, the assumption is not arbitrary as it sounds here, but mathematically deduced.

Corrected as follows 'These equations are solved by deducing a solution based on the form of the variables in Eq. (33), Eq. (34) and Eq. (35) above. The coefficients within this solution can then be determined, with respect to the boundary conditions, by substitution. This is 'solution by induction'. (Line 414)

8668, line 18: The meaning of the ε 's should be explained.

These are explained in the supplement, but the explanation will be moved to the main body text. (Line 462)

8670: lines 12-13: Reformulate.

The original formulation 'Although the shortwave radiation measurements are measured in the two components, the longwave radiation measurements are not.' was reformulated as follows: 'Although the upwelling and downwelling components shortwave radiation components were recorded at the field site (using a set of directional radiometers), only the downwelling component was recorded for the longwave radiation.' (Line 605)

8670, line 15: the standard technique uses the vegetation (and eventually soil layer), not the above canopy temperature. But it will be a reasonable approximation we think, at least for daytime . . .

Such a measurement is not available for the long term dataset, so we have to use the above canopy temperature instead, which seems to be the common practice for many sites where such a measurement is lacking. (c.f. Park et al, 'Estimation of surface longwave radiation components from ground-based historical net radiation and weather data', JGR 2008). We added the following explanation: 'Ideally vegetation temperature should be used, however, in the absence of such observations longwave radiation can be estimated from above canopy temperature as was reported to be a reasonable approximation (Park et al. 2008).

8671: Line 9: photosynthesis from ORCHIDEE: is this used for your calculations? It is stated in the following that the stomatal conductance is calculated independent from the ORCHIDEE values.

The original manuscript, as submitted, was intended as a basic set-up to demonstrate the multi-layer approach. For that purpose we tried to keep some aspects of the model i.e. photosynthesis and stomatal conductance as simple as possible. However, based on the comments mainly made by reviewer 2 we concluded that these simplifications did not help, contrary, they seemed to cause confusion. In the revised manuscript we make use of an updated version of the model that has been fully integrated in ORCHIDEE-CAN and therefore makes use of the ORCHIDEE-CAN photosynthesis, albedo and multi-layer stomatal conductance. This more complete approach is explained in the manuscript in Section 3.2 and Section 3.3.

8671: Line 13: The motivation for choosing basic options is unclear. There are several advantages in choosing the ORCHIDEE options (they are based on more extended knowledge, and the new modelling is intended to be added to the ORCHIDEE calculations). For the LAD, using an observed profile as is done here, is indeed logical.

See previous response

8671, line 24: ?recalculated?: re- formulate the sentence in terms of ?distribution over height?.

Following the full implementation of the multilayer albedo scheme, which is limited to 10 levels of vegetation, we replace with the following sentence: 'It is effectively LAI (m² per m²) per canopy levels, and thus has units of m² per level of the canopy ' (Line 645)

8672, line 6: 'negative' should be 'positive' ?

Yes, changed to 'positive radiation flux' (moved to Introduction, Line 38)

8672, lines 12-17: this is a strange logic. If the energy imbalance is 7.5% at the site, that is the value to stick to. Not the general 20% of Wilson et al.

Accepted (sentence removed) - we agree that we should describe the specific site.

8672, lines 17-18: 'are ..indicate': please correct sentence.

Underestimation of the data and mismatches exceeding the closure gap very likely indicate a shortcoming in the model (Line 670)

8672: Line 25-26 : Use of air temperature instead of radiative temperature may cause systematic errors.

Added as a possible explanation for the discrepancy (Line 680)

8672, line 27: On what is this conclusion based?

A portion of the upwelling longwave radiation is sourced from temperature changes in fluxes from the soil model, and the rest from the vegetation. So if the daytime surface layer temperature and heat storage is underestimated by the model, we expect reduced net longwave predicted to that which is measured, and vice versa for the nighttime scenario. This reasoning has been added to the manuscript (Line 680).

8673, lines 6-7: shouldn't the bias be called positive/negative if modeled values are higher/lower than observed? Here it is the other way round.

Agreed, corrected (Line 689)

8673, l21-23. It would be nice to show that this is the case, by executing a run with changes in stomatal conductances. Now we just have to believe this assertion.

This has been attempted in the revised manuscript, with a new formulation of stomatal conductance

8674, line 8: 'positive gradient': what is meant by this? $\delta T/\delta z$ is clearly negative.

Sign error corrected (Line 718)

8674, line 10: similar remark (the discussion has it OK).

Sign error corrected (Line 719)

8674, line 17: 'the current parameterization' versus 'numerical limitation': what's the difference ? A point of discussion is if it is possible to better simulate turbulence using a Lagrangian approach, which is not attempted here, as it is out of scope to maintain the implicit coupling technique, hence 'numerical limitation'.

The wording is clarified (line 727)

8675, line 2: '54' wrong number ?

Updated for new runs (Line 749)

8675 l4 and further. I do not really understand why observed profiles are given as individual ones and the modeled as a mean. Why cannot you show either means or the measured and modeled profiles at the same time. I also miss a little the discussion on night time stability in the canopy or may decoupling of the understory from the atmosphere above, that may lead to the night time problems.

Observed profiles are also provided as means in the plots, for a direct comparison. However the graphs were becoming crowded when all individual profiles both measured and simulated plotted, so we have switched to mean profiles and standard deviation for both the modelled and mean case (Fig 7).

8675: line 6: what is 'rolling average'?

It's an equivalent term to 'moving average'. We changed the text to 'moving average' (Line 742)

8675, line 9: has shown ← has been shown.

Corrected (Line 760)

8675, lines 13-14: 'It is likely therefore': this is a strange logic. A wrong albedo would explain a wrong sum of H + LE, not a wrong distribution of energy of H and LE (which accounts for the numerical 'offset'). See also comment 8675 l 21-23.

Accepted, we have removed this conjecture. (Line 765)

8676, lines 14- 15: strange sentence...

rephrased as: 'The transport closure model used here can be compared to the previous single-layer approach within ORCHIDEE. (Line 790)

8677, line 24: 'realm': 'scope'?

Accepted, 'scope' is the standard term to use here (Line 822)

8691, table 2: why is $R(\tau)$ taken as a constant, whereas on page 8662 it is a complicated function ?

It is a complicated function, but in fact depends only on one variable, which I the ratio of tau to T.L, the Lagrangian timescale (see Figure 2 of Makar et al, 1999). As such, after explaining the function, we can follow the approach of Stroud et al. (2005) and Wolfe et al. (2011), and apply R(tau) directly as a

constant. This simplification is now explained in the text (Line 327)

8691: table 3: the big change in the albedo is conspicuous . . .

We have now implemented the multi-layer albedo scheme, so the figures in this table no longer apply, as the albedo is no longer a tuning coefficient, but derived directly from the LAI profile. (Table 1)

8694: figure 3: the colors indicated in the legend are missing.

Size reduction made the colours hard to distinguish. This has been resolved in the new plot. (Figure 3)

8695, figure 4b and d: why isn't the null-line used for the horizontal line?

The horizontal line represents the overall mean of the year long run. This is now explained in the caption (Figure 4)

8695: figure 4: 'rolling'?

This is an equivalent term to 'moving average' and been changed accordingly (Figure 4).

8698-8699: 'gradients' → 'profiles'.

Accepted and updated (Figure 7)

General comments on the supplement

The supplement is explicit and sometimes over- explicit (e.g. the pieces on potential enthalpy (S1) and general balance formulation (S8-9) contain well-known information and could easily be deleted).

We opt to keep this information for readers with less of a background in Physics and Mathematics. It also serves as a transparent and clearly expressed documentation for the source code, which would otherwise be very difficult to follow.

Concerning the parts on 'induction' (S14-20) and boundary conditions (S21-30), the equations contain very much repetition; why not, when formulating the implicit problem (S13), express relations between unknowns using simple coefficients whose values are expressed once and for all into the known variables, and then continue (S14-S20) with the relations expressed into these coefficients? Similar remarks hold for the piece on the boundary conditions. By such efforts, a thorough abridgment should be possible. Checking signs in the balances is important! In Eq. S2.14 and S2.28 and the next one, the sensible and latent heat

in the right hand side are expressed with wrong signs. A similar problem occurs with ϕ_H and ϕ_{LE} in Eqs. S3.1-2. We agree with the reviewer that increasing the level of details made this section overly long, but we hope that its level of detail will pay off for future developers of the multi-layer energy budget. It is much easier for anyone interested in the process to follow than if they have to complete intervening steps to follow. Also, abridgement of the supplement will mean that errors such as the above (which, alongside many other errors, came to light during the coding process but, in this instance, not updated in the documentation) could not so easily be highlighted and resolved.

We agree that the approach is a little unconventional compared to standard derivations, but by setting out the derivation in this way we go some way to satisfy the wishes of the reviewer that 'we would like a confirmation of the authors that the results have been checked for exact agreement with all the original balance equations'. Sign error in fluxes were corrected, as in the case to the main text, as referred to above.

An easy alternative for the 'induction' The following point may come late, but may deserve attention as it would make reading the supplement a lot easier. The three equations for each layer i , expressing relations between the air temperature T_a , leaf temperature T_L and specific humidity q_a for the central layer and layers above and below, can be expressed in matrix form as $-A(i) u(i+1) + B(i) u(i) + C(i) u(i-1) = D(i)$ (i) in which u is the vector with unknowns (T_a, q_a, T_L) , A , B and C are known matrices, and D is a known vector. The notation is as in Eq. 11.7 in Richtmyer and Morton (RM) to which the authors refer. The components of A , B , C and D are already given in equations S2.29-S2.31 in the supplement. However, it is easy to eliminate T_L from the equations since it can be expressed in T_a and q_a of the same layer, so (i) can be reduced to a system in only two dimensions. In the following we take the equation in the latter sense. Now, the problem is to solve the equations simultaneously for all layers, with boundary conditions above and below. If (for the time being) boundary conditions on one side only are imposed on the solution, there will be a whole set of possible solutions but all of them subject to a recurrent relation $u(i) = E(i) u(i+1) + F(i)$ (ii) corresponding to Eq. 11.10 in RM, with E a matrix and F a vector which remain to be determined. The relation follows from general principles (linearity, two parameter family). To find E and F , one can follow the procedure of RM: substitute (ii) into (i) and derive $E(i) = \text{inv}(B(i) - C(i) E(i-1)) * A(i)$ (iii) $F(i) = \text{inv}(B(i) - C(i) E(i-1)) * (D(i) + C(i) * F(i-1))$ (as RM Eq. 11.11. There is a sign error in the book, whereas Eq. 8.23 for the scalar case was correct). From this, E and F can be calculated 'by induction' by starting from the boundary conditions on one side (first sweep). Then using E and F , one can determine u ($= (T_a, q_a)$) from (ii), starting with the boundary conditions on the other side (second sweep). These few lines, copied from RM, solve the 'induction problem' to which the Supplement spends six rather hard-to-digest pages now (S14- S19). Concerning the boundary conditions: it is possible to express the lower boundary conditions in the form $U(0) = E(0) u(1) + F(0)$ (with $u(0) =$

(TS, qS) and $u(1) = (Ta,1, qa,1)$, in which $E(0)$ is a known matrix and $F(0)$ a known vector. From this, the other $E(i)$ and $F(i)$ can be solved by induction (iii), going upward. Thereafter, the values of u_i can be solved, starting from the upper boundary conditions and going downward with (ii) above. These steps require no further explanation. In this way, the ten-page explanation about the boundary conditions could be drastically shortened!

The reviewer is correct that the technique outlined in Richtmyer & Morton does indeed represent a starting point to what is an alternative approach to solving the set of equations as outlined. We are grateful for this suggestion, and have provided a note of reference to this in the text (RM itself is already referenced the manuscript). Adopting this notation could be a way to abbreviate the derivation, though in the same way omission of the intervening steps in our derivation would also drastically shorten the supplementary material. However, we think that the purpose of the supplementary material should be both a comprehensive explanation for readers of the main text, and a documentation support for users of the source code, and without a full derivation as we have outlined potential users would otherwise have to write out the derivation themselves in order to check its validity. Furthermore, the alternative derivation assumes a good level of familiarity with the notation of RM, which readers of the paper from outside the numerical modelling sphere may not have. Finally, we aim to provide a link to the existing single layer implicit approach outlined in Polcher et al. (1998) and Best et al. (2004), as a form of continuation towards the new approach, and so prefer to retain their form of notation when possible.

Minor comments (supplement)

Try to reformulate Eqs. S2.21 and S2.24 without using second order derivatives. You use the difference between the flux above and below. The re-expression is not used, and it is incorrect if k has a layer-dependent value ($(d/dz)(k dT/dz)$ is not $k (d^2/dz^2) T$ etcetera).

We find the formulae are best expressed using second-order derivatives, but we have clarified the provenance of ‘ k ’ in the manuscript (Section S2.2).

Page 14: fill in the reference to Richtmyer and Morton.

Bug in the LaTeX compilation for references, now fixed (Section S3.9).

Page 21: S3.1 line 4: conflicts with the table above.

Typing error corrected (Section S4.1)

Page 22, top: do ϕ_H and ϕ_{LE} pertain to time t or $t+1$?

They pertain to ‘ $t+1$ ’ and a subscript is added for clarity (Equation S4.7).

Page 26 below: How is kS parameterized ? Solutions for ε are given in S3.50-S3.53, but these parameters are defined only later in Eqs. S3.58-59.

This sequence has been re-ordered, and some commentary added (Section S4.2).

Anonymous Referee #2

Received and published: 18 January 2015

General Comments

The authors proposed a multi-layer land surface energy model which is a part of ORCHIDEE-CAN. Multi-layer canopy models are theoretically robust compared to big leaf models; however the required computational resources hindered the use of multi-layer canopy models in GCMs. With the advancement in computing powers, it is possible to adopt multi-layer canopy model in GCMs and I am glad to see the authors chose this direction in their canopy modeling.

After reading this manuscript, several main comments appeared as follows:

1) The research gap and the novelty of this new scheme should be clearly stressed. There are a series of multi-layer energy balance models (e.g. (Norman, 1982; Wang Jarvis, 1990; Baldocchi Meyers, 1998; Alton et al., 2007)), and the current version did not successfully express the difference from the previous models.

We felt that the difference had been stressed sufficiently in the paper, but in hindsight this important innovation could indeed be emphasised more strongly and clearly, so we have added some text in the introduction to do this (Line 88): 'Where stand-alone surface models have few computational constraints, the typical applications of an Earth System Model (ESM) require global simulations at a spatial resolution of $2^\circ \times 2^\circ$ or a higher spatial resolution for century long time scales. Such applications come with a high computational demand that must be provided for by using a numerical scheme that can run stably over longer time steps (approx. 15 to 30 minutes), and that can solve a coupled or inter-dependent set of equations 95 without iterations. In numerics, such a scheme is known as an implicit solution, and requires that all equations in the coupled systems are linearised. Given that ORCHIDEE is the land surface model of the IPSL (Institute Pierre Simon Laplace) ESM, the newly developed multi-layer model was specifically designed in a numerically implicit way.'

2) In page 8671 (4.3. Model set-up), the authors used Jarvis type stomata conductance model and exponential extinction of light as function of LAI, which were different from ORCHIDEE-CAN. The authors argued these modifications were needed to only testing the performance of the multi-layer model, rather than ORCHIDEE-CAN. I do not agree with this. To better evaluate multi-layer energy balance model, then it is essential to couple water, energy and carbon fluxes across the multi-layers. I strongly recommend evaluating the multi-layer

model coupled to ORCHIDEE-CAN, which seems available in the companion manuscript to Naudts et al. (2014) (in review).

This innovations are available in the version of ORCHIDEE-CAN as documented in Naudts et al (2014), but not whilst the energy budget model was under development. We have now implemented both the multi-level albedo scheme and the updated stomatal conductance scheme, and re-written the text to reflect this. This full integration of the multi-layer energy budget into ORCHIDEE-CAN is the main reason of the substantial delay in addressing the review comments and presenting a revised manuscript.

To my mind, the key points in the multi-layer energy budget model include realistic simulations of 1) radiative transfer in PAR, NIR and LW, 2) leaf temperatures in sunlit and shade leaves for each layer, 3) separation of diffuse and beam components of radiative transfer, and 4) turbulent transfers across the layers, which are all included in most multi-layer canopy models. In the manuscript, the authors used total SW radiative transfer rather than separating PAR and NIR. Furthermore, the authors used fixed gap fraction and extinction coefficient regardless of solar zenith angles, which should cause fundamentally incorrect, unrealistic simulation of SW radiative transfer (i.e. Gap fraction= $\exp(-L \cdot k(\theta) \cdot \omega(\theta))$ where L is leaf area index, k is extinction coefficient, ω is clumping index, and θ is view zenith angle). Fixed value of extinction coefficient regardless of beam or diffuse radiation is also unrealistic. The authors should maximize the benefits in using multi-layer canopy model. How to get the realistic simulation of multi-layer energy budget without right canopy radiative transfer?

The primary aim of this work was to achieve the structural form of a canopy model that was capable of running stably when coupled to the atmosphere, and then work on improvements to the parameterisation of this model. The originally submitted paper achieved this as it was able to demonstrate a simulation that runs stably and efficiently, and produced realistic output of fluxes. However, some of the criticism raised by the reviewer has been dealt with while fully integrating the multi-layer energy budget into ORCHIDEE-CAN. To respond to each point:

1) The measurements available at this field site were SW radiation (which encompassed both PAR and NIR) and LW radiation. PAR and NIR measurements are indeed available for selected field campaigns, and we understand why such measurements would be useful, particularly in terms of photosynthesis. This is probably a second order problem, but a future version of the model can be used to distinguish between distribution of PAR and NIR, for scenarios when such measurements are available.

2) With regards to sunlit and shaded leaves - within a layer all leaves are treated in the same way but when moving from the top to the bottom of the canopy leaves receive more diffuse light compared to direct light. This change with

depth is a first-order effect of the impact of sun versus shaded leaves. ORCIDEE-CAN calculates photosynthesis every half hours and therefore photosynthesis is one of the speed-limiting processes. Distinguishing sunlit and shaded leaves for each level would double the computation time of a speed-limiting process and thus substantially slow down the model (which is not a problem for a single site but becomes a problem when regional, continental or global simulation are run typically on over 5000 pixels. Large scale simulation are the main objective of ORCHIDEE-CAN). Further improving the simulation of photosynthesis itself is not a current priority of the ORCHIDEE-team because other processes are known to be less well modelled. Nevertheless, within canopy chemistry would be a good justification to separate shade/sunlit leaves but this is a future development.

3) In the multilayer albedo scheme (McGrath et al, in prep), we have been able to separate the diffuse and direct components of radiative transfer. This has been explained in the manuscript (Section 3.9)

4) Turbulent transfer is indeed included in most multi-layer canopy models, and the technique we have outlined here represents a compromise between speed of operation and simulation of the unique aspects, such as counter-gradient fluxes. In the light of point 2 of this reply, finding an implicit solution for the near-field far-field approach by Raupach appears rather high on the priority list.

Leaf temperatures should be computed by solving a set of equations that include leaf energy balance, transpiration, stomata conductance, and leaf boundary layer resistance. I do believe Jarvis type stomata model is not relevant here as demonstrated by ‘stomata suicide’ in the early version of SiB (Randall et al., 1996; Sellers et al., 1997; Berry, 2012).

The leaf energy balance is already calculated in the model, and we have now updated the stomata conductance parameterisation following the approach by Ball and Berry 1987. This is explained in the model in Section 3.9

Leaf boundary layer resistance should be improved. The authors did not include Grasshof number which reflects the buoyancy of air when temperature difference between leaf and air is large. I believe this is likely an important factor at Tumbarumba site which experiences very dry season but Eucalyptus trees still hold the leaves.

The review alights on a possible expansion to the model here ? the Grasshof number can be used in situations of free convection in the canopy to improve the simulation of the boundary layer resistance, and is an area we could return to in studies in which leaf temperature has been recorded. This development would require substantial future work, beyond the scope of this first demonstration paper, but it is further point of potential improvement of the model.

The multi-layer energy budget model should separate sunlit and shade components at each layer. This was already made several decades ago by Norman, Baldocchi, etc. In a non-dense canopy like Tumbarumba site, beam radiation can penetrate deeper into the canopies, and it is well possible to have sunlit leaves in the deeper canopy. Sunlit and shade leaves have substantially different light loading (beam does not change across canopy depths, but diffuse radiation is exponentially decreased with canopy depths), different leaf temperature, different stomata conductance, photosynthesis, thus latent heat flux and sensible heat flux.

The model as presented in the revised document now implements the multi-layer albedo model that has been developed by McGrath et al (in prep), which builds on Pinty et al (2006), who developed a sophisticated two stream system to allow for canopy gaps and structure in the calculation of light that is absorbed, transmitted or reflected by each layer of the canopy. So the light penetration is now more sophisticated than in the originally submitted paper, as detailed in Section 3.9.

However, the proposal here is to divide each layer of the canopy further into a fraction that is subject to direct light exposure and a fraction of only indirect light exposure. Such a step was considered in the design of the model, and could obviously require two separate temperatures for each canopy layer, and, for consistency, two separate surface temperatures as well. Should we then take the mean surface temperature as representative? Or should these two surface temperatures be retained between time steps? The former case results in an almost equivalent situation to the multi-layer model as presented, where the radiation incident to each level is assumed uniform. In the latter case we create what amounts to two separate leaf temperature columns and two soil surface layers (each of these columns shares a common surrounding atmospheric temperature and humidity, and hence transport between the layers is shared). This is a possible scenario for extension to the model, alongside the concept of multiple columns for multiple PFTs. Ultimately the objective of a model such as ORCHIDEE-CAN is not to simulate an individual site but to model large areas (5000 pixels with each pixels between 3 to 20 PFTs). Computation time and computer memory constrain all of our developments.

The longwave radiative transfer is very important but less explored part in the previous studies. I hoped to find something new in this manuscript, but the authors very simply described by citing LRTM model. The longwave radiative transfer model should be sensitive to leaf temperature; however, I could not find how the leaf temperature was computed in the manuscript. In open canopy like Tumbarumba site, forest floor temperature could be pretty high during dry seasons, thus lower part of canopy could get higher amount of LW from the floor. I am curious how the proposed scheme dealt with LW budget in each canopy layer influenced by the forest floor.

The leaf temperature is calculated using the leaf energy budget in the model (equation 13 in the original submitted manuscript). The simulation is based around the LRTM of Gu et al (1999), but we have added a more complete description of the scheme in the revised manuscript, including the relationship to radiation from the forest floor. The simulation of leaf temperature is a very interesting study in itself (particularly with regards to compound emission, as featured in the discussions for future applications), but we have no direct measurements of leaf temperature for the field site featured here. This was added to the manuscript (Section 7), as inspiration for future developments.

3) Although I recognize the high quality dataset at Tumbarumba site, I am not sure whether this site alone could be used to test the multi-layer energy budget model. There was no data in longwave radiation. There was no radiation data in the forest floor. Thus it seems hard to evaluate the proposed scheme thoroughly. For example, in the Yatir forest flux tower site in Israel, people measured SW and LW components of radiation above the canopy and above the forest floor (Rotenberg Yakir, 2011). Air and skin surface temperature profiles across the canopy depths were also measured.

The Tumbarumba site was originally chosen as comprehensive measurement data was readily available, even though some measurements were missing ? an issue with most in-canopy datasets. The objective of this manuscript was to describe the mathematical derivation of an implicit multi-layer energy budget and show that the initial implementation can more or less reproduce observed fluxes and profiles in a sparse canopy (because that is where the big leaf model is most likely to fail). These objectives already resulted in an extensive manuscript such that it was decided to prepare a follow-up manuscript in which a set of eight diverse forest sites (though not including Yatir, for which we did not obtain measurement data at the time of the work), for which detailed data is available, is being used to parameterise the model in more detail (Chen et al, in prep).

Specific comments:

P8650 L14: tha → the

corrected

P8650 L15: Define LMDz

Definition from section 2 has been moved up the document to first mention of LMDz here (line 14).

P8653: I recommend adding two-leaf model which split canopy into sunlit and shaded leaves (Sinclair et al., 1976; dePury Farquhar, 1997; Ryu et al., 2011), and a 3-D canopy radiative transfer model coupled with 1D turbulence scheme (Kobayashi et al., 2012).

As discussed in the reply to Reviewer 1, above, the two-leaf model proposal is a feasible extension project for the model, though we are satisfied that the performance at present proves that the model, as designed, is capable of simulating canopy fluxes in a more physically realistic form than was the case with the single layer model. The implementation of sunlit and shaded leaves in the column could be a further improvement, in tandem with the implementation of separate land use columns within the same atmospheric model grid square. Computational constraints means that we should start with a reasonable level of complexity for a model that is designed to be run on a global scale, and some compromises have to be made in this regard. We now include the multi-layer albedo scheme of McGrath et al (in prep) that accounts for canopy structure and gaps, solar zenith angle and direct and diffuse light interactions thus providing an efficient but improved short wave radiation scheme. The 1-D turbulence scheme (Massman and Weil, 1999) is part of the multi-layer energy budget.

P8654 L10: ‘simulates’ → ‘Simulates’

corrected

P8654 L15: I recommend removing ‘in preparation’ citation (McGrath et al., 2014)

This is a key development, so the refernence is retained ? we cite as as (McGrath et al., in prep)

P8655 L11: Define IPSL

Institute Pierre Simon Laplace (added, at first occurence, in abstract line 100)

P8656 L25: Before starting with a series of equations, please explain why the leaf vapor pressure assumption is important and how this component is related to other key processes. Also, do you want to compute vapor pressure or specific humidity at the leaf? Two variables have different units and physical meanings. The tile includes vapor pressure, but the equations in this section are related to specific humidity. Apparently, this section aims to compute specific humidity at leaf surface, which can be calculated as follows (Garratt, 1992): $q=0.622*Ea/(Pressure-0.378*Ea)$ where Ea is actual vapor pressure, and pressure is atmospheric pressure. As leaf is saturated, Ea is the saturated vapor pressure at the leaf temperature. Saturated vapor pressure at certain temperature can be approximated using Clausius-Clapeyron relation (Henderson-Sellers, 1984). To me, computing specific humidity at leaf surface is pretty simple and straightforward; whereas, the authors used a set of complicated equations, which could be simplified.

This section has been simplified (section 3.1).

P8656 L27: The vapor pressure of the leaf \rightarrow does it mean vapor pressure at the leaf surface, or within the leaf?

It's the vapour pressure within the leaf. This has been clarified in the manuscript (Line 183).

P8659 L6: Is there any special reason in using R_b , rather than R_i ? In L6, the authors defined $R_b=R_i$, then why not using R_i instead of R_b ? As there are too many symbols, please try to remove redundant symbols.

We used this notation for simplicity during the derivation. R_i denotes resistance per level, as it is important to stress that this value is level independent, and are defined in lines 221 and 225.

P8659 L8: I wonder why the authors used Jarvis type stomatal conductance model, which is too empirical. Ball-Berry or Medlyn models coupled photosynthesis and stomata conductance, which is much more relevant in the proposed multi-layer model as stomata, photosynthesis, transpiration, and leaf energy balance can be all coupled. Jarvis type model does not allow to couple those processes. Is there any specific reason to use Jarvis type stomata model? If yes, then please explain. Also, include the equation of stomata conductance in the manuscript. This is so important equation.

The reason was to provide a simple to implement function for testing of the model. This has now been upgraded to the Ball-Berry approach in the revised manuscript and model. A more complete reply to this comment is provided in the response to reviewer 1, above.

P8660 L10: In Eq 13, the key variable is the leaf temperature (TL). Please explain how you computed leaf temperature. I am curious how leaf temperature could be computed accurately by using Jarvis type stomata conductance model.

Leaf temperature was computed using the leaf layer energy balance, as described in section 3.3 of the manuscript. The form of stomatal conductance parameterisation may effect the accuracy of this calculation, though the Jarvis model that is reported in the original manuscript did produced realistic values. The re-submitted manuscript applies a Ball-Berry scheme for stomatal conductance. The lack of studies of leaf temperature within forest canopies (we are aware of Guenther et al., 1996, Helliker & Richter, 2008) precludes a more thorough assessment of this part of the model. Leaf temperature is calculated as laid out, in section 3.

P8670 L12: Define the 'two components'

Upwelling and downwelling LW radiation - clarified in the text (Line 626).

P8670 L14: Please describe how the canopy temperature was measured. Canopy temperature depends on sun-target-sensor geometry, and the location of target.

In fact we use here the above canopy temperature. Within canopy temperature was available within the canopy for the short-term campaign, but not for the long term measurements. The site and original field study is described in more detail in Haverd et al. (2009), as referenced.

P8670 L26: heatflux → heat flux

Corrected (Line 638)

P8671: Now I see the authors made assumptions in stomata conductance and radiative transfer.

The method is outlined in section 4.3 have been updated in the revised manuscript

P8679 L1: I am curious how the model computed leaf temperature, which should be coupled with photosynthesis, transpiration, stomata conductance, and importantly aerodynamic resistance.

Leaf temperature was computed using the leaf layer energy balance, as described now in section 3.4 of the manuscript. All of the factors listed above are taken into account in this calculation

P8679 L12: I might miss, but where did you describe the computation of soil temperature?

The lower boundary condition for this model is T_{surf} , the surface temperature (equation 484). We have added the following description to the manuscript: ‘The interaction with the soil temperature is by means of the soil flux term J_{soil} . Beneath the soil surface layer, there is a seven layer soil model (Hourdin 1992) which is unchanged from the standard version of ORCHIDEE.’

Table 3: Canopy gap fraction and SW extinction coefficient were fixed to 0.4. This assumption made me very confused. Both variables are actually very sensitive to solar zenith angle. Why such incorrect assumptions were needed given the use of sophisticated multi-layer energy balance model? Practically, 0.4 of extinction coefficient for SW is too low.

The albedo scheme has now been updated to the multi-level model, and is documented in the revised manuscript. The gap fraction is calculated from the tree height, tree diameter and specific leaf area assuming spherical shaped canopies.

A more detailed description of these processes can be found in Naudts et al. (2015).

Anonymous Referee #3

Received and published: 26 January 2015

The authors motivate this manuscript with a very important point: that land surface models give highly divergent responses to land-cover change; that this relates to out-dated and poorly documented parameterizations of canopy processes; and that multi-layer canopy models that explicitly resolve non-linearities within the plant canopy are a necessary step forward to improve the models and better represent the consequences of land-cover change. I strongly agree with this view. However the paper, as currently written, does not represent that step forward. 1. The advantage of multi-layer canopy models over big-leaf models is that they resolve gradients of radiation, leaf temperature, stomatal conductance, and energy fluxes within the canopy. These models emphasize radiative transfer, distinguishing visible and near-infrared wavebands, scattering within the canopy, the different absorption of direct beam and diffuse radiation, and the differences between sunlit and shaded leaves. There is no discussion of these key features of multi-layer canopy models, so when I see model biases I am left to wonder how much is due to the radiative transfer. Similarly, the authors use a very outdated stomatal conductance model. Would a better stomatal conductance model have improved the simulations?

As discussed in response to the other reviewers, above, the two-leaf model proposal is a feasible extension project for the model, though we are satisfied that the performance at present proves that the model, as designed, is capable of simulating canopy fluxes in a more physically realistic form than was the case with the single layer model. The implementation of sunlit and shaded leaves in the column could be a further improvement, in tandem with the implementation of separate land use columns within the same atmospheric model grid square. Computational constraints means that we should start with a reasonable level of complexity for a model that is designed to be run on a global scale, and some compromises have to be made in this regard.

We now include the multi-layer albedo scheme of McGrath et al (in prep) that accounts for canopy structure and gaps, solar zenith angle and direct and diffuse light interactions thus providing an efficient but improved short wave radiation scheme.

We have introduced an improved calculation of stomatal conductance. The multi-layer model as described in the previous version of the article applied the light-dependent formulation of Lohanner et al. (1980), after Jarvis (1976). It was originally intended as a means to evaluate the balance and stability of the model before the implementation of a more complete scheme. We have now

replaced this with the scheme of Ball et al. (1987).

2. Instead of discussing the critical features of a multi-layer canopy model and how that class of models is an improvement over big-leaf models, this manuscript instead emphasizes the numerical implementation of an implicit temperature calculation. There is no emphasis on physiological and micrometeorological processes in the canopy. Much of the text and equations derive and justify the implicit temperature calculation. Again, when I see biases in the simulations I cannot judge whether these are due to process details or to the numerical scheme.

We agree that the original paper did not include sufficient information on the physiological and micro-meteorological processes in the canopy, so we have provided a duller description here. The initial goal was to test the feasibility of a multi-layer energy budget simulation in a global model as we believe that this is the significant innovation (the first type of model to do this suitable for coupling to an atmospheric model). We wanted to emphasise what makes this particular model unique? that it can be coupled to an atmospheric model without large amounts of run-time to multiple iterations, and short time-steps. However, we have now updated the parameterisation of several physiological aspects of the model, and both the outcome of this and a fuller documentation are provided in the updated manuscript.

3. The longwave radiative transfer seems to be separate from the implicit temperature calculation. This is very poorly explained and the few details provided are buried in the supplementary materials. Again, this is one of the key features of a multi-layer canopy: how do you couple longwave radiative transfer (which depends on leaf temperature) to the leaf temperature calculation.

The original manuscript did include references relating to the scheme that we have used, but we have now provided more detail here.. A fuller description of the long-wave radiative transfer scheme is provided in the revised manuscript (section 3.8).

4. Some additional key details are missing: a description of soil fluxes (net radiation, latent heat, sensible heat, heat storage); there is no mention of canopy interception and evaporation.

As explained to reviewer #1 and #2, these aspects are inherited from the existing ORCHIDEE model. This has been clarified in the manuscript with more precise references (Line 483)

5. The presentation of the model is confusing. The fundamental equations being solved are (13), (24), and (28). These are given very deep into the manuscript. Instead, the initial description of the model emphasizes calculation of specific

humidity (Eq. 2-10) and its linearization with respect to temperature. This is not the key feature of the model. It would be better to first present the leaf temperature, canopy air temperature, and canopy specific humidity equations. Then describe these, their derivation, and their numerical implementation in more detail.

We felt it best to outline the initial conditions and assumptions behind the model first, as is convention. Some of these details have now been abbreviated, with further detail moved to the supplementary material, so as not to distract from the principal, innovative parts of the work.

6. The description of the model, equations, and variables is sloppy. Here are some examples, and there are many more:

We have comprehensively revised the presentation of the equations and variables, beyond the errors brought to light in the review process

(i) Eq. (11) has the variable Dz but the following text refers to Ds ; $df(z)$ is unexplained.

The description of the leaf boundary layer resistance has been revised in the updated manuscript (section 3.2).

(ii) Eq. (20) introduces $R(\tau)$ to calculate the eddy diffusivity in the canopy. I immediately wonder how the parameter τ is defined. Only much later in the manuscript do I find that Eq. (20) is not used at all; instead $R(\tau)$ is set to a constant.

It is a complicated function, but in fact depends on only one variable, which is the ratio of τ to T_L , the Lagrangian timescale (see Figure 2 of Makar et al, 1999). As such, after explaining the function, we apply $R(\tau)$ as a constant directly.

(iii) Table 1 is not a complete list of model variables. This table has now been updated to include all of the model variables, in alphabetical order, and grouped by alphabet type.

(iv) Some variables have the same notation; e.g., TL represents both leaf temperature and the Lagrangian timescale. Leaf temperature symbol changed to T_{leaf} . T_L for the Lagrangian timescale retained out of convention.

(v) R_i is called stomatal resistance in section 3.2, whereas R_l is the leaf boundary layer resistance. However, the use of R_i in Eq. (13) to calculate latent heat flux implies that this also includes the leaf boundary layer resistance for water vapor. Or is the leaf boundary layer resistance not included in the latent

heat flux equation? Table 1 does not help explain, because both R_i and R'_i are called ‘stomatal resistance for sensible and latent heat flux, respectively’. What is ‘stomatal resistance for sensible heat’?

The terms R_i and R'_i are used here to simplify the mathematical derivation of the implicit energy budget model by avoiding even more terms of the relevant equations. The boundary layer resistance for water vapour is included in the R'_i , in series with the stomata conductance. We have updated the parameterisation of the latter, and provide further information about the calculation of the former beyond the existing references in each case. The term ‘stomatal resistance for sensible heat’ has been corrected (section 3.2)

7. How would a more advanced stomatal model that couple photosynthesis (Farquhar model) and stomatal conductance (Ball-Berry) work in the implicit temperature calculation? That model requires leaf temperature to calculate photosynthetic parameters (e.g., V_{cmax}) and vapor pressure deficit. This can be easily done in an iterative leaf temperature calculation. How would it be done in an implicit temperature calculation?

We have implemented the above approach (that is to say the Farquhar model, with Ball-Berry) in the revised manuscript, but do we use the leaf temperature from the previous time step. This was done in order to avoid introducing large complications to the implicit scheme, and keeping in mind the need to linearise the dependence of V_{cmax} on temperature. A potential future refinement would be to apply an ‘operator split’ approach (e.g. analogous to that which is used in the model of Stroud et al. (2005) for diffusion and chemistry operators).

A multi-layer land surface energy budget model for implicit coupling with global atmospheric simulations

James Ryder¹, Jan Polcher², Philippe Peylin¹, Catherine Ottlé¹, Yiying Chen¹,
Eva van Gorsel³, Vanessa Haverd³, Matthew J. McGrath¹, Kim Naudts¹,
Juliane Otto^{1,4}, Aude Valade¹, and Sebastiaan Luyssaert¹

¹Laboratoire des Sciences du Climat et de l'Environnement (LSCE-IPSL, CEA-CNRS-UVSQ),
Orme des Merisiers, 91191 Gif-sur-Yvette, France

²Laboratoire de Météorologie Dynamique (LMD, CNRS), Ecole Polytechnique, 91128 Palaiseau,
France

³CSIRO Oceans & Atmosphere Flagship, 2 Wilf Crane Cr., Yarralumla, ACT 2600, Australia

⁴now at: Climate Service Center 2.0, Helmholtz-Zentrum Geesthacht, Hamburg, Germany

Correspondence to: James Ryder (jryder@lsce.ipsl.fr)

Abstract. In Earth system modelling, a description of the energy budget of the vegetated surface layer is fundamental as it determines the meteorological conditions in the planetary boundary layer and as such contributes to the atmospheric conditions and its circulation. The energy budget in most Earth system models has ~~long~~ been based on a 'big-leaf approach', with averaging schemes that represent in-canopy processes. ~~Furthermore, to be stable, that is to say, over large time steps and without large iterations, a surface layer model should be capable of implicit coupling to the atmospheric model.~~ Such models have difficulties in reproducing consistently the energy balance in field observations. ~~We here outline a newly developed numerical model for energy budget simulation, as a component of the land surface model ORCHIDEE-CAN (Organising Carbon and Hydrology In Dynamic Ecosystems - CANopy).~~ This new model implements techniques from single-site canopy models in a practical way. It includes representation of in-canopy transport, a multilayer longwave radiation budget, height-specific calculation of aerodynamic and stomatal conductance, and interaction with the bare soil flux within the canopy space. Significantly, it avoids iterations over the height of ~~the~~ the canopy and so maintains implicit coupling to the atmospheric model LMDz ([Laboratoire de Météorologie Dynamique Zoomed model](#)). As a first test, the model is evaluated against data from both an intensive measurement campaign and longer term eddy covariance measurements for the intensively studied Eucalyptus stand at Tumbarumba, Australia. The model performs well in replicating both diurnal and annual cycles of [energy and water](#) fluxes, as well as the ~~gradients of vertical gradients of temperature and of~~ sensible heat fluxes. ~~However, the model overestimates sensible heat flux against an underestimate of the radiation budget. Improved performance is expected through~~

~~the implementation of a more detailed calculation of stand albedo and a more up-to-date stomatal conductance calculation.~~

1 Introduction

Earth system models are the most advanced tools to predict future climate (Bonan, 2008). These
25 models represent the interactions between the atmosphere and the surface beneath, with the surface formalized as a combination of open oceans, sea-ice and land. For land, a description of the energy budget of the vegetated surface layer is fundamental as it determines the meteorological conditions in the planetary boundary layer and as such contributes to the atmospheric conditions and its circulation.

30 The vegetated surface layer of the Earth is subject to incoming and outgoing fluxes of energy, namely atmospheric sensible heat (H , Wm^{-2}), latent heat (LE , Wm^{-2}), shortwave radiation from the sun (R_{SW} , Wm^{-2}), longwave radiation (R_{LW} , Wm^{-2}) emitted from other radiative sources such as clouds and atmospheric compounds and soil heat exchange with the subsurface (GJ_{soil} , Wm^{-2}). The sum of these fluxes is equal to the amount of energy that is stored or released
35 from the surface layer over a given time period Δt (s). So, for a surface of overall heat capacity C_p ($JK^{-1}m^{-2}$) the temperature change over time, ΔT , is described as:

$$C_p \frac{\Delta T}{\Delta t} = H + LE + R_{LW} + R_{SW} - H - \lambda E + GJ_{soil} \quad (1)$$

The sign convention used here makes all upward fluxes positive (so a positive sensible or latent heat flux from the surface cools the ground). Likewise a positive radiation flux towards the surface
40 warms the ground.

One key concept in modelling the energy budget of the surface Eq. (1) is the way in which the surface layer is defined. In many cases the surface layer describes both the soil cover and the vegetation above it as a uniform block. Such an approach is known as a ‘big leaf model’, so called because the entirety of the volume of the trees or crops and the understorey, as well as the surface layer,
45 are simulated in one entity, to produce fluxes parameterised from field measurements. In the model under study, named ORCHIDEE-CAN (Organising Carbon and Hydrology In Dynamic Ecosystems - CANopy) (Naudts et al., 2015) (Naudts et al., 2014), the land surface is effectively simulated as an ‘infinitesimal surface layer’ - a conceptual construct of zero thickness. As demonstrated in the original paper describing this model, such an approach, whilst reducing the canopy to simple components, was nevertheless able to simulate surface fluxes to an acceptable degree of accuracy for the
50 sites that were evaluated as the original SECHIBA (Schematic of Hydrological Exchange at the Biosphere to Atmosphere Interface) model (Schulz et al., 2001) and later as a component of the original ORCHIDEE model (Krinner et al., 2005), precursor to the basis of ORCHIDEE-CAN.

The proof that existing land to surface simulations may now be inadequate comes from inter-
55 comparison studies, such as Pitman et al. (2009), which evaluated the response of such models to

land use change scenarios. That study found a marked lack of consistency between the models, an observation they attributed to a combination of the varying implementation of LCC (Land Cover Change) maps, the representation of crop phenology, the parameterisation of albedo and the representation of evapotranspiration for different land cover types. Regarding the latter two issues, the models they examined did not simulate in a transparent, comparable manner the changes in albedo and evapotranspiration as a result of changes in vegetation cover, such as from forest to cropland. It was not possible to provide a definitive description of the response of latent heat flux to land cover change across the seven models under study, because there was substantial difference in the mechanisms which describe the evaporative response to the net radiation change across the conducted simulations.

Furthermore, the latent and sensible heat fluxes from off-line land surface models were reported to depend very strongly on the process-based parameterisation, even when forced with the same micro-meteorological data (Jiménez et al., 2011). The structure of land surface models, it has been suggested (Schlosser and Gao, 2010), may be more important than the input data in simulating evapotranspiration. Hence, improvements to the soil-surface-atmosphere interaction (Seneviratne et al., 2010), and to the hydrology (Balsamo et al., 2009), are considered essential for better simulating evapotranspiration. We can therefore assert that refinements in the numerical schemes of land surface models represent a logical approach to the further constraint of global energy and water budgets.

Large scale validation, therefore, has revealed that the 'big leaf approach' has difficulties in reproducing fluxes of sensible and latent heat (Jiménez et al., 2011; Pitman et al., 2009; de Noblet-Ducoudré et al., 2012) for a wide range of vegetated surfaces. This lack of modelling capability is thought to be due to the 'big leaf approach' not representing the vertical canopy structures in detail and thus not simulating factors such as radiation partition, separation of height classes, turbulent transport within the vegetation and canopy-atmosphere interactions - all of which are crucial factors in the improved determination of sensible and latent heat flux estimates (Baldocchi and Wilson, 2001; Ogée et al., 2003; Bonan et al., 2014), as well as the presence of an understorey, or mixed canopies, as is proposed by Dolman (1993). Furthermore, a model that is able to determine the temperatures of elements throughout the canopy profile will provide for a more useful comparison with remote sensing devices, for which the 'remotely sensed surface temperature' also depends on the viewing angle. (Zhao and Qualls, 2005, 2006)

This gap in modelling capability provides the motivation for developing and testing a new, multi-layer, version of the energy budget simulation based on Eq. (1). A multi-layer approach is expected to model more subtle but important differences in the energy budget in relation to multi-layer vegetation types such as forests, grasses and crops. Through the simulation of more than one canopy layer, the model could simulate the energy budget of different plant types in two or more layers such as found in savannah, grassland, wood species and agro-forestry systems (Verhoef and Allen, 2000; Saux-Picart et al., 2009)

95 Where stand-alone surface models have few computational constraints, the typical applications of an Earth System Model (ESM) require global simulations at a spatial resolution of $2^\circ \times 2^\circ$ or a higher spatial resolution for century long time scales. Such applications come with a high computational demand that must be provided for by using a numerical scheme that can run stably over longer time steps (~15 to 30 minutes), and that can solve a coupled or interdependent set of equations without iterations. In numerics, such a scheme is known as an implicit solution, and requires that all equations in the coupled systems are linearised. Given that ORCHIDEE is the land surface model of the IPSL (Institute Pierre Simon Laplace) ESM, the newly developed multi-layer model was specifically designed in a numerically implicit way.

2 Model requirements

Several alternative approaches to the big leaf model have been developed. These alternatives share the search for a more detailed representation of some of the interactions between the heat and radiation fluxes and the surface layer. Following Baldocchi and Wilson (2001), the range and evolution of such models includes:

1. the big-leaf model (e.g. Penman and Schofield (1951))
2. the big-leaf with dual sources (e.g. Shuttleworth and Wallace (1985))
3. two layer models which split the canopy from the soil layer (e.g. Dolman (1993); Verhoef and Allen (2000); Yamazaki et al. (1992))
4. three layer models, which split the canopy from the soil layer, and simulate the canopy as a separate understorey and overstorey (e.g. Saux-Picart et al. (2009))
5. ~~1D~~ one-dimensional multi-layer models (e.g. Baldocchi and Wilson (2001))
6. ~~3D~~ three-dimensional models that consist of an array of plants and canopy elements (e.g. Sinoquet et al. (2001))

For coupling to an atmospheric model (see below), and thus running at a global scale, simplicity, robustness, generality and computational speed need to be balanced. We therefore propose a ~~1D~~ one-dimensional multi-layer model combined with a ~~statistical-detailed~~ description of the ~~3D canopy~~ three-dimensional canopy characteristics. We aim for a multi-layer canopy model that:

- 120 – ~~Simulates~~ simulates processes that are sufficiently well understood at a canopy level such that they can be parameterised at the global scale through (semi-)mechanistic, rather than empirical, techniques. Examples of such processes are the description of stomatal conductance (Ball et al., 1987; Medlyn et al., 2011), and the partition of radiation in transmitted, reflected and absorbed radiation at different canopy levels (Pinty et al., 2006; McGrath et al., in prep.)

- 125 – ~~Simulates~~ simulates the exposure of each section of the canopy, and the soil layer, to both shortwave and longwave radiation. At the same time the model should also simulate in-canopy gradients, separating between soil-surface - atmosphere and vegetation - atmosphere interactions
- ~~Simulates~~ simulates non-standard canopy set-ups, for instance combining different species
- 130 in the same vertical structure, e.g. herbaceous structures under trees, as explored by Dolman (1993); Verhoef and Allen (2000); Saux-Picart et al. (2009)
- ~~Describes~~ describes directly the interaction between the soil surface and the sub-canopy using an assigned soil resistance rather than a soil-canopy amalgamation
- ~~Is~~ is flexible, that is to say sufficiently stable to be run over fifty layers or over just two, i.e. the
- 135 soil-surface and the canopy
- ~~Avoids introducing interactions~~ avoids introducing numerics that would require iterative solutions.

Where the first five requirements relate to the process description of the multi-layer model, the last requirement is imposed by the need to couple ORCHIDEE to an atmospheric model. Generally,

140 coupling an implicit scheme will be more stable than an explicit scheme, which means that it can be run over longer timesteps. Furthermore, the approach is robust: for example, if there is an instability in the atmospheric-land surface model, it will tend to be dampened in subsequent timesteps, rather than diverge progressively. For this work, the model needs to be designed to be run over time steps as long as 30 minutes in order to match the timesteps of the IPSL atmospheric model, ~~called~~

145 LMDz (Laboratoire de Mtorologie Dynamique Zoom model; Hourdin et al. (2006)) LMDz, to which it is coupled, and so to conserve processing time. However, the mathematics of an implicit scheme have to be linearised and is thus by necessity rigidly and carefully designed. As discussed in Polcher et al. (1998) and subsequently in Best et al. (2004), the use of implicit coupling was widespread in models when the land surface was a simple bucket model, but as the land surface schemes have in-

150 creased in complexity, explicit schemes have, for most models, been used instead, because complex explicit schemes are more straightforward to derive than implicit schemes. As they demonstrate, there is nevertheless a framework for simulating all land-surface fluxes and processes (up to a height of, say, 50 m, so including above canopy physics) in a tiled 'non-bucket' surface model coupled, using an implicit scheme, to an atmospheric model.

155 3 Model description

We here summarise the key components of ~~a~~ the new implicit multi-layer energy budget model. The important innovation, compared to existing multi-layer canopy models that work at the local scale

(e.g. Baldocchi (1988); Ogée et al. (2003)), is that we will solve the problems implicitly - i.e. all variables are described in terms of the ‘next’ timestep. The notation used here is listed in full in
160 Table 1, and is chosen to complement the description of the LMDz coupling scheme, as is described in Polcher et al. (1998). A complete version of the derivation of the numerical scheme is provided in the supplementary material.

We propose to regard the canopy as a network of potentials and resistances, as shown in Figure 1, a variation of which was first proposed in Waggoner et al. (1969). At each level in the network we
165 have the state variable potentials: the temperature of the atmosphere at that level, the atmospheric humidity and the leaf level temperature. We include in the network fluxes of latent heat and sensible heat between the leaves at each level and the atmosphere, and vertically between each canopy level. The soil surface interacts with the lowest canopy level, and uppermost canopy level interacts with the atmosphere. We also consider the absorption and reflection of radiation by each vegetation layer and
170 by the surface (SW and LW) and emission of radiation (LW only). This represents the ‘classic’ multi-layer canopy model formulation, with a network of resistances that ~~stimulate~~ simulate the connection between the soil surface temperature and humidity, and fluxes passing through the canopy to the atmosphere.

The analogy is the ‘circuit diagram’ approach, for which T_a and q_a represent the atmospheric
175 ‘potentials’ of temperature and specific humidity at different heights and H and ~~LE~~ λE are the sensible and latent heat fluxes that act as ‘currents’ for these potentials. At each level within the vegetation, T_a and q_a interact with the leaf level temperature and humidity T_L and q_L through the resistances R_i (for ~~aerodynamic resistance~~ resistance to sensible heat flux) and R'_i (for ~~stomatal resistance~~ resistance to latent heat flux). The change in leaf level temperature is determined by the
180 energy balance at each level.

The modelling approach formalises the following constraints and assumptions.

3.1 Leaf vapour pressure assumption

We assume that the air within leaf level cavities is completely saturated. This means that the vapour pressure of the leaf can be calculated as the saturated vapour pressure at that leaf temperature (Mon-
185 teith and Unsworth, 2008). Therefore the change in pressure within the leaf is assumed proportional to the difference in temperature between the present timestep and the next one, multiplied by the rate

of change in saturated pressure against temperature.

$$q_0 \equiv q_{L,leaf,i}^{t+1} = q_{sat} \frac{\partial q_{sat}}{\partial T} \bigg|_{T_{L,i}^t, T_{leaf,i}^t} (T_{L,leaf,i}^{t+1} - T_{L,leaf,i}^t) \quad (2)$$

$$= \frac{\delta q_{sat}}{\delta T} \frac{\partial q_{sat}}{\partial T} \bigg|_{T_{L,i}^t, T_{leaf,i}^t} (T_{L,leaf,i}^{t+1}) + \left(q_{sat} \frac{\partial q_{sat}}{\partial T} \bigg|_{T_{L,i}^t, T_{leaf,i}^t} - T_{L,leaf,i}^t \frac{\delta q_{sat}}{\delta T} \frac{\partial q_{sat}}{\partial T} \bigg|_{T_{L,i}^t, T_{leaf,i}^t} \right) \quad (3)$$

$$= \alpha_i T_{L,leaf,i}^{t+1} + \beta_i \quad (4)$$

where α_i and β_i are regarded as constants for each particular level and timestep, so $\alpha_i = \frac{\delta q_{sat}}{\delta T} \bigg|_{T_{L,i}^t}$

$$\text{and } \beta_i = \left(q_{sat} \frac{\partial q_{sat}}{\partial T} \bigg|_{T_{L,i}^t, T_{leaf,i}^t} - T_{L,leaf,i}^t \frac{\delta q_{sat}}{\delta T} \frac{\partial q_{sat}}{\partial T} \bigg|_{T_{L,i}^t, T_{leaf,i}^t} \right)$$

To find a solution we still need to find an expression for the terms $q_{sat} \frac{\partial q_{sat}}{\partial T} \bigg|_{T_{L,i}^t, T_{leaf,i}^t}$ and $T_{L,leaf,i}^t \frac{\delta q_{sat}}{\delta T} \frac{\partial q_{sat}}{\partial T} \bigg|_{T_{L,i}^t, T_{leaf,i}^t}$ in α_i and β_i above.

Using the empirical approximation of Tetens (e.g., Monteith and Unsworth, 2008, 2.1) and the specific humidity vapour pressure relationship we can describe the saturation vapour pressure to within 1 Pa up to a temperature of about 35°C.

$$e_{sat}(T) = e_{sat}(T^*) \exp[A(T - T^*) / (T - T')]$$

where $A = 17.27$, $T^* = 273\text{K}$, $e_{sat}(T^*) = 0.611 \text{ kPa}$, $T' = 36\text{K}$

Specific humidity is related to vapour pressure by the relationship: (e.g., Monteith and Unsworth, 2008, 2.1):

$$q = \frac{\left(\frac{M_W}{M_A} \right)}{(p - e) + \left(\frac{M_W}{M_A} \right) e}$$

where q = specific humidity (kg/kg), e = vapour pressure (kPa), (M_W/M_A) = (ratio of molecular weight of water to air) = 0.622, and p = atmospheric pressure (kPa)

To find $q_{sat}^{T_{L,i}^t}$, we substitute $e_{sat}(T_L)$ derived from for e in:

$$q_{sat}^{T_L} = \frac{\left(\frac{M_W}{M_A} \right)}{(p - e_{sat}(T_L)) + \left(\frac{M_W}{M_A} \right) e_{sat}(T_L)}$$

To calculate $\frac{\delta q_{sat}}{\delta T} \bigg|_{T_{L,i}^t}$, we use the expression for the saturated humidity curve against temperature (as derived using the method of Monteith and Unsworth (2008)):

$$q_{sat}^{T_{L,i}^t} = q_0 e^{-\lambda M_W / RT}$$

into:

$$\frac{\delta q_{sat}}{\delta T} |_{T_{L,i}^t} = \frac{\lambda M_W}{R(T_{L,i}^t)^2} \left(\frac{\left(\frac{M_W}{M_A} \right)}{(p - e_{sat}(T_L)) + \left(\frac{M_W}{M_A} \right) e_{sat}(T_L)} \right)$$

Thus the specific humidity of the leaf follows a relationship to the leaf temperature that is described by a saturation curve.

215 3.2 Derivation of the leaf layer resistances (R_i and R'_i)

The variables R_i and R'_i represent the leaf layer resistance, in our circuit diagram analogue, resistances to the sensible and latent heat flux, respectively.

The resistance to the sensible heat flux, that we refer to as R_i , is calculated based upon the leaf, is equal to the boundary layer resistance, and is described according to the following expression from

220 Baldocechi (1988): $R_{b,i}$, of the leaf surface:

$$R_i = R_{b,i} \quad (5)$$

For sensible heat flux, $R_{b,i}$ is calculated as:

$$R_{b,i} = \frac{d_l}{D_{h,air} \cdot Nu} \quad (6)$$

for which $D_{h,air}$ is the heat diffusivity of air and d_l is the characteristic leaf length.

225 The Nusselt number, Nu , is calculated as in (Grace & Wilson, 1976) for which:

$$R_b(z) Nu = \frac{l}{df(z) D_z Sh(z)} 0.66 Re^{0.5} Pr^{0.33} \quad (7)$$

where R_b denotes the boundary layer resistance ($= R_i$), l is the characteristic length of leaves, D_s is the molecular diffusivity of the entity in question, Pr is the Prandtl number (which is 0.70 for air), and Re is the Reynolds number, for which:

$$230 Re = \frac{d_l u}{\mu} \quad (8)$$

where μ is the kinematic viscosity of air ($= 0.15 \text{ cm}^2 \text{ s}^{-1}$), d_l is again the characteristic dimension of the leaf and u is the wind speed at the level i in question.

The resistance to latent heat flux is calculated as the sum of the boundary layer resistance (which is calculated slightly differently) and the leaf stomatal resistance:

$$235 R'_i = R'_{b,i} + R_{s,i} \quad (9)$$

In this case we use the following expression:

$$R_{b,i} = \frac{d_l}{D_{h,H_2O} \cdot Sh} \quad (10)$$

in which D_{h,H_2O} is the heat diffusivity of water vapour and Sh is the Sherwood number, as calculated in Baldocchi (1988). R'_i is the stomatal resistance of the leaf that is calculated using the method of Lohammer et al. (1980), after Jarvis (1976), but there is potential for a more up-to-date parameterisation such as that of Medlyn et al. (2011) which for laminar flow is:

$$Sh = 0.66 Re^{0.5} Sc^{0.33} \quad (11)$$

and for turbulent flow is:

$$Sh = 0.03 Re^{0.8} Sc^{0.33} \quad (12)$$

for which Sc is the Schmidt number. The transition from laminar to turbulent flow takes place in the model when the Reynolds number exceeds a value of 8000 (Baldocchi, 1988).

The stomatal conductance, $g_{s,i}$ is calculated according to the Ball-Berry approximation, per level i . In summary:

$$g_{s,i} = LAI_i \left(g_0 + \frac{a_1 A h_s}{C_s} \right) \quad (13)$$

where g_0 is the residual stomata conductance, A the assimilation rate, h_s the relative humidity at the leaf surface and C_s the concentration of CO_2 at the leaf surface.

This is one of three simultaneous equations for the stomatal conductance, which is tied to the demand and supply of CO_2 in the leaf. The description here is related to that of the standard Orchidee model (e.g., LSCE/IPSL, 2012, 2.1), for which the g_s that is used to determine the energy budget is calculated as an amalgamated value, over the sum of all levels i . However, in this new energy budget description we keep separate the g_s for each level i , and use the inverse of this conductance value to determine the resistance that is $R_{s,i}$. Furthermore, the amount of water that is supplied to the plant is calculated, both at the soil and leaf level (Naudts et al., 2014). In times of drought, the water supply term may be lower than the theoretical latent flux than can be emitted for a certain g_s , using equation Eq. (29). In these cases, the g_s term at leaf level is restricted to that corresponding to the supply term limited latent heat flux at the level in question.

3.3 Leaf interaction with precipitation

Both soil interactions and leaf level evaporation components are parameterised using the same interception and evaporation coefficients as are used in the existing ORCHIDEE model (Krinner et al. (2005); LSCE/IPSL (2012)), extended by ORCHIDEE-CAN. Notably, ORCHIDEE-CAN assumes horizontal clumping of plant species, and hence canopy gaps, as opposed to the uniform medium that is applied

in the original ORCHIDEE. A portion of rainfall is intercepted by the vegetation (i.e. a canopy interception reservoir), as determined by the total canopy LAI and by the PFT, where it will be subject to evaporation as standing water. The rest falls on the soil surface, and is treated in the same way as for bare soil in the existing model.

3.4 The leaf energy balance equation for each layer

For vegetation, we assume the energy balance is satisfied for each layer. We extend Eq. (1) in order to describe a vegetation layer of volume ΔV_i , area ΔA_i and thickness Δh_i :

$$\Delta dV_i \theta_i \rho_v \frac{\delta T_{L,i}}{\delta t} + \frac{dT_{leaf,i}}{dt} = (H_i + LE_i + R_{SW,i} + R_{LW,i} - H_i - \lambda E_i) \Delta A_i \quad (14)$$

All terms are defined in Table 1. The **heat capacity-specific heat** of each vegetation layer $(\Theta_i) - (\theta_i)$ is assumed equal to that of water, and is modulated according to the Leaf Area Density (m^2/m^3) at that level. Since the fluxes in the model are described per square metre, ΔA_i may be represented by the Plant Area Density ($PAD, m^2/m^3$) for that layer, where ‘plant’ denotes leaves, stems, grasses or any other vegetation included in **optical** Leaf Area Index (LAI) measurements. Note that LAI, that has units of m^2/m^2 , is a value that describes the integration over the whole of the canopy profile of PAD (which is applied per metre of height, hence the dimension m^2/m^3). Canopy layers that do not contain foliage may be accounted for at a level by assigning that $R_i = R'_i = \infty$ for that level (i.e. an open circuit).

Rewriting **equation 8** Eq. (14) in terms of the state variables and resistances that are shown in Figure 1 means that R_i is the resistance to sensible heat flux and R'_i the resistance to latent heat flux. Dividing both sides of the equation by ΔV_i , the volume of the vegetation layer (equal to Δh_i multiplied by ΔA_i), expresses the sensible and latent heat fluxes between the leaf and the atmosphere **respectively as:**

$$(a) \quad \theta_i \rho_v \frac{\delta T_{L,i}}{\delta t} + \frac{dT_{leaf,i}}{dt} = \left(\Theta_{p,a} R_{SW,i} + R_{LW(tot),i} - C_p^{air} \rho_a \frac{(T_{L,ileaf,i} - T_{a,i})}{R_i} - \lambda \rho_a \frac{(q_{L,ileaf,i} - q_{a,i})}{R'_i} + R_{SW,i} + R_{LW(tot),i} \right) \Delta A_i \quad (15)$$

n.b. this is the first of three key equations that are labelled (a), (b) or (c) on the left hand side, throughout.

3.4.1 Vertical transport within a column

3.5 Vertical transport within a column

The transport equation between each of the vegetation layer segments may be described as:

$$\frac{\delta(\rho\chi)}{\delta t} + \frac{d(\rho\chi)}{dt} + \text{div}(\rho\chi u) = \text{div}(\Gamma \text{grad}(\chi)) + S_\chi \quad (16)$$

where div is the operator that calculates the divergence of the vector field, χ is the property under question, ρ is the fluid density, u is the horizontal wind speed vector (~~assumed negligible here~~), S_χ is the concentration for the property in question and Γ is a parameter that will in this case be the diffusion coefficient $k(z)$.

300 To derive from this expression the conservation of scalars equation, as might be applied to vertical air columns, we proceed according to the Finite Volume Method, as used in the FRAME (Fine Resolution Atmospheric Multi-pollutant Exchange; Singles et al. (1998)) model and as outlined in Vieno (2006) and derived from Press (1992). The final equation is specific to a ~~1D~~ one-dimensional model, and so does not include a term of the influence of horizontal wind. The resulting expression
305 is sufficiently flexible to allow for variation in the height of each layer, but we preserve vegetation layers of equal height here for simplicity:

$$\frac{\delta \chi}{\delta t} \frac{d\chi}{dt} \Delta V = \frac{k(z) \frac{\delta d^2 \chi}{\delta z^2} \Delta A + S(z) \Delta V}{\delta z} \frac{d}{dz} \left(k(z) \frac{\delta \chi}{\delta z} \frac{d\chi}{dz} \right) \Delta A + S(z) \Delta V \quad (17)$$

$$= \frac{\delta}{\delta z} \frac{d}{dz} (F(z)) \Delta A + S(z) \Delta V \quad (18)$$

310 where F is the vertical flux density, z represents coordinates in the vertical and x coordinates in the streamwise direction. χ may represent the concentration of any constituent that may include water vapour or heat, but also gas or aerosol phase concentration of particular species. S represents the source density of that constituent (in this case the fluxes of latent and sensible heat from the vegetation layer), and the transport $k(z)$ term represents the vertical transport between each layer.

315 In the equation above, we substitute the flux-gradient relationship according to the expression:

$$F(z) = -k(z) \frac{d\chi}{dz} \quad (19)$$

$$F(z) = -k(z) \frac{\delta \chi}{\delta z}$$

This approach allows future applications to include a supplementary term to simulate emissions or deposition of gas or aerosol based species using the same technique.

320 The transport ~~term/terms~~, per level i in the vertically discretised form, ~~k_i is are~~ calculated using the 1D second-order closure model of Massman and Weil (1999), which makes use of the LAI profile of the stand. ~~Their model provides profiles~~ Fuller details are outlined in that paper, but the in-canopy windspeed is dependent on C_{Def} , the effective phytoelement canopy drag coefficient. This is defined according to Wohlfahrt and Cernusca (2002) :

$$325 \quad C_{Def} = a_1^{-LAD/a_2} + a_3^{-LAD/a_4} + a_5 \quad (20)$$

where LAD is the Leaf Area Density and a_1, a_3 and a_5 are parameters to be defined.

This second-order closure model also provides profiles of σ_w , the standard deviation in vertical velocity and T_L , the Lagrangian timescale within the canopy. The eddy diffusivity term T_L is defined as in the model of Raupach (1989a) and represents the time, since 'emission' at which an emitted flux transitions from the near field (emitted equally in all directions, and not subject to eddy diffusivity), and the far field (which is subject to normal eddy diffusivity and gradient influences). The eddy diffusivity $k_i(z)$ is then derived in the far-field using the expressions from Raupach (1989b):

$$k_i = \sigma_{w,i}^2 T_{L,i} \quad (21)$$

However, the simulation of near field transport in canopies is more complex, and requires ideally a Lagrangian solution (Raupach, 1989a). As that is not directly possible in this implicit solution, we instead adopt a method developed by Makar et al. (1999) (and later Stroud et al. (2005) and Wolfe and Thornton (2010)) for the transport of chemistry species in canopies for which a 'near-field' correction term R -factor R_{nf} is introduced to the far-field solution, and is expressed as follows:-

$$R(\tau) = \frac{(1 - e^{-\tau/T_L})(\tau/T_L - 1)^{3/2}}{(\tau/T_L - 1 + e^{-\tau/T_L})^{3/2}}$$

where which is based on the ratio between the Lagrangian timescale T_L and τ , which represents the time since emission for a theoretical near-field diffusing cloud of a canopy source, as defined in Raupach (1989a) which, unlike for the far-field, acts as point source travelling uniformly in all directions. In fact the expression for R_{nf} depends ultimately on the ratio of T_L and τ , rather than their absolute values. As there is a direct relationship between the ratio τ and R_{nf} (Figure 2 of Makar et al. (1999)), we here tune the model directly with R_{nf} , as a proxy for τ/T_L . R_{nf} appears to depend on canopy structure and on venting (Stroud et al., 2005), but has yet to be adequately described.

There is thus a modified expression for k_i , with R - R_{nf} acting effectively as a tuning coefficient for the near-field transport:

$$k_i^* = R_{nf}(\tau) \sigma_{w,i}^2 T_{L,i} \quad (22)$$

The necessity to account for the near-field transport effect in canopies, and in particular open canopies, remains a question under discussion (McNaughton and van den Hurk, 1995; Wolfe and Thornton, 2010).

3.5.1 Fluxes of sensible and latent heat between each atmospheric layer the canopy layers

We re-write the scalar conservation equation (expression for scalar conservation (Eq. (??), above), as applied to canopies, as a pair of expressions for the fluxes of sensible and latent heat (so, comparing with Eq. (??), $\chi \equiv T$ or q , $F \equiv H$ or $LE - \lambda E$ and $S \equiv$ (the source sensible or latent heat flux at each vegetation layer)).

Neither the sensible or latent heat flux profile is constant over the height of the canopy. The rate
 360 of change of $T_{a,i}$ (the temperature of the atmosphere surrounding the leaf at level i) and $q_{a,i}$ (the
 specific humidity of the atmosphere surrounding the leaf at level i) are proportional to the rate of
 change of the respective fluxes with height and the source of heat fluxes from the leaf at that level:

$$(b) \quad \underbrace{\Theta_{p,a}}_{\rho_a} \underbrace{C_p^{air}}_{\rho_a} \underbrace{\frac{\delta T_{a,i}}{\delta t}}_{\frac{dT_{a,i}}{dt}} \Delta V_i = - \underbrace{\frac{\delta H_{a,i}}{\delta z}}_{\frac{dH_{a,i}}{dz}} \underbrace{\Delta V_i}_{\Delta V_i} + \left(\frac{T_{L,i,leaf,i} - T_{a,i}}{R_i} \right) \left(\frac{\Theta_{p,a} \rho_a \underbrace{C_p^{air}}_{\rho_a}}{\underbrace{\Delta h_i}_{\Delta h_i}} \right) \Delta V_i$$

now we assume the flux-gradient relation and so write Eq. (19) according to sensible heat flux at
 365 level i , $H_{a,i}$:

$$H_{a,i} = -(\rho_a \Theta_{p,a} C_p^{air}) k_i \frac{\delta T_{a,i}}{\delta z} * \frac{dT_{a,i}}{dz} \quad (24)$$

which is substituted in Eq. (23)

$$(b) \quad \boxed{\frac{dT_{a,i}}{dt} \Delta V_i = \frac{d^2(k_i^* T_{a,i})}{dz^2} \Delta V_i + \left(\frac{T_{leaf,i} - T_{a,i}}{R_i} \right) \left(\frac{1}{\Delta h_i} \right) \Delta V_i} \quad (25)$$

and in exactly the same format following the same approach for the expression for latent heat flux at
 370 level i , $\underline{LE}_{a,i} = \lambda E_{a,i}$:

$$(\underline{LE} \lambda E)_{a,i} = -(\lambda \rho_a) k_i \frac{\delta q_{a,i}}{\delta z} * \frac{dq_{a,i}}{dz} \quad (26)$$

which is, again, substituted in Eq. (23):

$$(c) \quad \lambda \rho_a \frac{\delta dq_{a,i}}{\delta dt} \Delta V_i = - \frac{\delta d(\underline{LE} \lambda E)_{a,i}}{\delta dz} \Delta V_i + \left(\frac{q_{L,i} - q_{a,i}}{R'_i} \right) \left(\frac{\lambda \rho_a}{\Delta h_i} \right) \Delta V_i \quad (27)$$

$$= - \frac{\delta d(\underline{LE} \lambda E)_{a,i}}{\delta dz} \Delta V_i + \left(\frac{(\alpha T_{L,i,leaf,i} + \beta_i) - q_{a,i}}{R'_i} \right) \left(\frac{\lambda \rho_a}{\Delta h_i} \right) \Delta V_i \quad (28)$$

375

$$(c) \quad \boxed{\frac{\delta q_{a,i}}{\delta t} \frac{dq_{a,i}}{dt} \Delta V_i = k_i \frac{\delta^2 q_{a,i}}{\delta z^2} \frac{d^2(k_i^* q_{a,i})}{dz^2} \Delta V_i + \left(\frac{(\alpha T_{L,i,leaf,i} + \beta_i) - q_{a,i}}{R'_i} \right) \left(\frac{1}{\Delta h_i} \right) \Delta V_i} \quad (29)$$

We have now defined the three key equations in the model:

- eqn. (a) balances the energy budget at each vegetation-canopy air level
- eqn. (b) balances heat fluxes vertically between each vegetation level and ‘horizontally’ be-
 380 tween each vegetation level and the surrounding atmosphere-air
- eqn. (c) balances humidity fluxes in the same sense as for eqn. (b)

The equations must be solved simultaneously, whilst at the same time satisfying the limitations constraints of an implicit scheme.

3.5.2 Write equations in implicit format

385 The difference between explicit and implicit schemes is that an explicit scheme will calculate each value of the variable (i.e. temperature and humidity) at the next time step entirely in terms of values from the present time step. An implicit scheme requires the solution of equations that couple together values at the next time step. The basic differencing scheme for implicit equations is described by Richtmyer and Morton (1967). In that work, they introduce the method with an example equation:

$$390 \quad u^{t+1} = B(\Delta t, \Delta x, \Delta y)u_t^t \quad (30)$$

where B denotes a linear finite difference operator, Δt , Δx , Δy are increments in the respective co-ordinates and $u_t^t, u_{t+1}^t, u^{t+1}$ are the solutions at respectively steps 't' and 't+1'

It is therefore assumed that B depends on the size of the increments Δt , Δx , Δy and that, once known, it may be used to derive u_{n+1} from u_n u^{t+1} from u^t . So if B can be determined we can use this relationship to calculate the next value in the temporal sequence. However, we necessarily need to know the initial value in the sequence (i.e. u_0). This means that it is an 'initial value problem'. Now, the equivalent of eqn. (18) Eq. (30), in the context of a column model, such as LMDz, takes the form:

$$X_{li} = C_{li}^X + D_{li}^X X_{l-1, i-1} \quad (31)$$

400 This describes the state variable X (for example temperature) at level li , in relation to the value at level $l-1, C_{li}^X$ and D_{li}^X are coupling coefficients that are derived in that scheme. In this particular example, the value of $W_t W_i$ at time t is defined in terms of $X_{l-1, i-1}$ at the same timestep.

To maintain the implicit coupling between the atmospheric model (i.e. LMDz) and the land surface model (i.e. ORCHIDEE) we need to express the relationships that are outlined above in terms of a linear relationship between the 'present' timestep t and the 'next' timestep $t+1$. We therefore rewrite equations (a), (b) and (c) in implicit form (i.e. in terms of the 'next' timestep, which is $t+1$), as below: explained in the following subsections.

Implicit form of the energy balance equation:-

410 3.5.3 Implicit form of the energy balance equation

We substitute the expressions for leaf level vapour pressure Eq. (4) to the energy balance equation Eq. (15), which we rewrite in implicit form:

$$(a) \quad \theta_i \rho_v \frac{(T_{L,leaf,i}^{t+1} - T_{L,leaf,i}^t)}{\Delta t} = \left(\frac{1}{\Delta h_i} \right) \left(\Theta_{p,a} - C_p^{air} \rho_a \frac{(T_{L,leaf,i}^{t+1} - T_{a,i}^{t+1})}{R_i} + \lambda \rho_a \frac{(\alpha_i T_{L,leaf,i}^{t+1} + \beta_i - q_{a,i}^{t+1})}{R'_i} \right. \\ \left. + \eta_1 R_{LW}^{down} + \eta_2 T_{L,leaf,i}^{t+1} + \eta_3 + \eta_4 R_{SW}^{down} \right) \quad (32)$$

We difference-

3.5.4 Implicit form of the sensible heat flux equation

We differentiate Eq. (25) according to the finite volume method Eq. (17), and divide by ΔV_i :

420

$$(b) \quad \frac{T_{a,i}^{t+1} - T_{a,i}^t}{\Delta t} = k_i^* \left(\frac{(T_{a,i+1}^{t+1} - T_{a,i}^{t+1})}{\Delta z_i \Delta h_i} \right) - k_{i-1}^* \left(\frac{(T_{a,i}^{t+1} - T_{a,i-1}^{t+1})}{\Delta z_{i-1} \Delta h_i} \right) + \left(\frac{1}{\Delta h_i} \right) \frac{(T_{L,leaf,i}^{t+1} - T_{a,i}^{t+1})}{R_i} \quad (33)$$

~~We difference~~

425 3.5.5 Implicit form of the latent heat flux equation

We differentiate Eq. (29) according to the finite volume method Eq. (17), and divide by ΔV_i :

430

$$(c) \quad \frac{q_{a,i}^{t+1} - q_{a,i}^t}{\Delta t} = k_i^* \left(\frac{(q_{a,i+1}^{t+1} - q_{a,i}^{t+1})}{\Delta z_i \Delta h_i} \right) - k_{i-1}^* \left(\frac{(q_{a,i}^{t+1} - q_{a,i-1}^{t+1})}{\Delta z_{i-1} \Delta h_i} \right) + \left(\frac{1}{\Delta h_i} \right) \frac{(\alpha_i T_{L,leaf,i}^{t+1} + \beta_i - q_{a,i}^{t+1})}{R'_i} \quad (34)$$

430 3.5.6 Solution by induction

These equations are solved by ~~assuming a solution of a particular form and finding the coefficients that are introduced in terms of the coefficients of the layer above~~ deducing a solution based on the form of the variables in Eq. (32), Eq. (33) and Eq. (34) above. The coefficients within this solution can then be determined, with respect to the boundary conditions, by substitution. This is ‘solution by induction’.

435

With respect to Eq. (33), we wish to express $T_{a,i}^{t+1}$ in terms of values further down the column, to allow the equation to be solved by ‘moving up’ the column, as in Richtmyer and Morton (1967). There is also an alternative method to solve these equations also derived from that text, which we describe in the supplementary material.

440

In order to solve by implicit means, we make the assumption (later to be proved by induction) that:

$$i) \quad \boxed{T_{a,i}^{t+1} = A_{T,i} T_{a,i-1}^{t+1} + B_{T,i} + C_{T,i} T_{L,leaf,i}^{t+1} + D_{T,i} q_{a,i-1}^{t+1}} \quad (35)$$

445

$$ii) \quad \boxed{q_{a,i}^{t+1} = A_{q,i} q_{a,i-1}^{t+1} + B_{q,i} + C_{q,i} T_{L,leaf,i}^{t+1} + D_{q,i} T_{a,i-1}^{t+1}} \quad (36)$$

We then also re-write these expressions in terms of the values of the next level:

$$i) \quad \boxed{T_{a,i+1}^{t+1} = A_{T,i+1} T_{a,i}^{t+1} + B_{T,i+1} + C_{T,i+1} T_{L,leaf,i+1}^{t+1} + D_{T,i+1} q_{a,i}^{t+1}} \quad (37)$$

$$ii) \quad q_{a,i+1}^{t+1} = A_{q,i+1} q_{a,i}^{t+1} + B_{q,i+1} + C_{q,i+1} T_{L,i+1}^{leaf,i+1} + D_{q,i+1} T_{a,i}^{t+1} \quad (38)$$

450 where $A_{T,i}$, $B_{T,i}$, $C_{T,i}$, $D_{T,i}$, $A_{q,i}$, $B_{q,i}$, $C_{q,i}$ and $D_{q,i}$ are constants for that particular level and timestep and are, as yet, unknown, but will be derived. We thus substitute Eq. (35) and Eq. (37) into Eq. (33) to eliminate T_{t+1} . Symmetrically, we substitute Eq. (36) and Eq. (38) into Eq. (34) to eliminate q_{t+1} .

For the vegetation layer, we conduct a similar procedure, in which the leaf level temperature is described as follows (where E_i , F_i and G_i are known assumed constants for the level and timestep in question):

$$iii) \quad T_{leaf,i}^{t+1} = E_i q_{a,i-1}^{t+1} + F_i T_{a,i-1}^{t+1} + G_i \quad (39)$$

Now the coefficients $A_{T,i}$, $B_{T,i}$, $C_{T,i}$, $D_{T,i}$, $A_{q,i}$, $B_{q,i}$, $C_{q,i}$ and $D_{q,i}$ can be described in terms of the coefficients from the level above and the potentials (i.e. T and q) at the previous timestep, which we can in turn determine by means of the boundary conditions. So we have a set of coefficients that may be determined for each time-step, and we have the means to determine T_S (and q_S via the saturation assumption). We thus have a process to calculate the temperature and humidity profiles for each timestep by systematically calculating each of the coefficients from the top of the column (the ‘downwards sweep’) then calculating the ‘initial value’ (the surface temperature and humidity) and finally calculating each T_a , q_a and T_{leaf} by working up the column (the ‘upwards sweep’). The term $\frac{T_{L,i}^{t+1}}{T_{leaf,i}^{t+1}}$ can also be described in terms of the variables at the level below by $\frac{T_{L,i+1}^{t+1}}{T_{leaf,i+1}^{t+1}}$ using equation iii) and its terms E_i , F_i and G_i .

3.6 The boundary conditions

3.6.1 The upper boundary conditions

470 In stand-alone simulations, the top level variables $A_{T,n}$, $C_{T,n}$, $D_{T,n}$ and $A_{q,n}$, $C_{q,n}$, $D_{q,n}$, are set to zero and $B_{T,n}$ and $B_{q,n}$ set to the input temperature and specific humidity, respectively, for the relevant time step (as in Best et al. (2004)) In coupled simulations, $A_{T,n}$, $B_{T,n}$ and $B_{q,n}$, $C_{q,n}$ are taken from the respective values at lowest level of the atmospheric model. Table 2 summarises the boundary conditions for both the coupled and un-coupled simulations.

475 3.6.2 The lower boundary condition

We need to solve the lowest level transport equations separately, using an approach which accounts for the additional effects of radiation emitted, absorbed and reflected from the vegetation layers:

$$T_S^{t+1} = \frac{T_S^t + \frac{\Delta t}{\theta_0} (\eta_{1,S} R_{LW}^{down} + \eta_{3,S} + \eta_{4,S} R_{SW}^{down} + \xi_1 + \xi_3) - J_{soil}}{(1 - \frac{\Delta t}{\theta_0} (\xi_2 + \xi_4 + \eta_{2,S}))} \frac{T_S^t + \frac{\Delta t}{\theta_0} (\eta_{2,S} + \eta_{3,S} R_{SW}^{down} + \xi_1 + \xi_3 - J_{soil})}{(1 - \frac{\Delta t}{\theta_0} (\xi_2 + \xi_4 + \eta_{1,S}))}$$

(40)

where $\eta_{1,S}$, $\eta_{2,S}$, $\eta_{3,S}$ and $\eta_{4,S}$ and $\eta_{3,S}$ are components of the radiation scheme, and ξ_1 , ξ_2 , ξ_3 and ξ_4 are components of the surface flux (where $\phi_H = \xi_1 + \xi_2 T_s^{t+1}$ and $\phi_{LE} = \xi_3 + \xi_4 T_s^{t+1}$; refer to section 3.2 of the supplementary material).

3.7 The radiation scheme

The interaction with the soil temperature is by means of the soil flux term J_{soil} . Beneath the soil surface layer, there is a seven layer soil model (Hourdin, 1992) which is unchanged from the standard version of ORCHIDEE.

A partially implicit longwave radiation scheme was developed for the model, however, the combination of explicit and implicit terms in this scheme resulted in a slight imbalance in the radiation budget. In order to completely conserve energy, we instead make use of an alternative approach – the

3.7 Radiation scheme

The radiation approach is the application of the Longwave Radiation Transfer Matrix (LRTM) (Gu, 1988; Gu et al., 1999) –

This approach separates (Gu, 1988; Gu et al. 1999), as applied in Ogee et al. (2003). This approach separates the calculation of the radiation distribution completely from the implicit expression. Instead a single source term for the longwave long wave radiation is added at each level. This means that the distribution of radiation refers to the present time step, rather than the next. However is now completely explicit (i.e. makes use of information only from the ‘present’ and not the ‘next’ time step. However, an advantage of the approach is that it accounts for a higher order of reflections from adjacent levels than that the single order that is assumed in the alternative process process above.

The components for longwave radiation are abbreviated as:

$$R_{LW,i} = \eta_{1,i} T_{leaf,i}^{t+1} + \eta_{2,i} \quad (41)$$

The shortwave radiation component is abbreviated as:

$$R_{SW,i} = \eta_{3,i} R_{SW}^{down} \quad (42)$$

where $\eta_{1,i}$, $\eta_{2,i}$ and $\eta_{3,i}$ are components of the radiation scheme. $\eta_{1,i}$ accounts for the components relating to emission and absorption of LW radiation from the vegetation at level i (i.e. the implicit parts of the long wave scheme) and $\eta_{2,i}$ the components relating to radiation from vegetation at all other levels incident on the vegetation at level i (i.e. the non-implicit part of the long wave scheme).

$\eta_{3,i}$ is the component of the SW radiation scheme - it describes the fraction of the total downwelling short wave light that is absorbed at each layer, including over multiple forward- and back-reflections, as simulated by the multilayer albedo scheme (McGrath et al., in prep.). The fraction of original

510 downwelling SW radiation that is ultimately reflected from the surface and from the vegetation cover back to the canopy can then be calculated using this information.

3.8 The longwave radiation scheme

We applied a version of the Longwave Radiation Transfer Scheme of Gu (1988, 1999), with some modifications that are summarised here. The method assumes that scattering coefficients for longwave radiation are very small (of the order of 0.05), and can thus be ignored.

The basics of the scheme can be described by the matrix equation for a canopy of m levels:

$$\begin{pmatrix} \Delta N_{surf} \\ \Delta N_1 \\ \cdot \\ \cdot \\ \Delta N_m \\ \Delta N_{above} \end{pmatrix} = \begin{pmatrix} \alpha_{0,0}^{LW} & \alpha_{0,1}^{LW} & \cdot & \cdot & \cdot & \alpha_{0,m}^{LW} & \alpha_{0,m+1}^{LW} \\ \alpha_{1,0}^{LW} & \alpha_{1,1}^{LW} & \cdot & \cdot & \cdot & \alpha_{1,m}^{LW} & \alpha_{1,m+1}^{LW} \\ \cdot & & & & & & \cdot \\ \cdot & & & & & & \cdot \\ \cdot & & & & & & \cdot \\ \alpha_{m,0}^{LW} & \alpha_{m,1}^{LW} & \cdot & \cdot & \cdot & \alpha_{m,m}^{LW} & \alpha_{m,m+1}^{LW} \\ \alpha_{m+1,0}^{LW} & \alpha_{m+1,1}^{LW} & \cdot & \cdot & \cdot & \alpha_{m+1,m}^{LW} & \alpha_{m+1,m+1}^{LW} \end{pmatrix} \begin{pmatrix} \sigma(T_{surf}^t)^4 \\ \sigma(T_{leaf,1}^t)^4 \\ \cdot \\ \cdot \\ \sigma(T_{leaf,m}^t)^4 \\ R_{LW} \end{pmatrix}$$

520 for which each element $\alpha_{i,j}^{LW}$ is defined as:

$$\alpha_{i,j} = \begin{cases} -1, & i = j = 0. \\ \mathfrak{F}(\ell_i - \ell_{j-1}) - \mathfrak{F}(\ell_i - \ell_j), & i=0, j=1, 2, \dots, m \\ \mathfrak{F}(\ell_i), & i=0, j=m+1 \\ \mathfrak{F}(\ell_j - \ell_{i-1}) - \mathfrak{F}(\ell_{j-1} - \ell_{i-1}) - \mathfrak{F}(\ell_j - \ell_i) - \mathfrak{F}(\ell_{j-1} - \ell_i), & i=1, 2, \dots, m, j=1, 2, \dots, i-1 \\ 2\mathfrak{F}(\ell_i) - 2, & i=1, 2, \dots, m, j=i \\ \mathfrak{F}(\ell_i - \ell_{j-1}) - \mathfrak{F}(\ell_i - \ell_j) - \mathfrak{F}(\ell_{i-1} - \ell_{j-1}) - \mathfrak{F}(\ell_{i-1} - \ell_j), & i=1, 2, \dots, m, j=i+1, i+2, \dots, m \\ \mathfrak{F}(\ell_i), & i=m+1, j=0 \\ \mathfrak{F}(\ell_j) - \mathfrak{F}(\ell_{j-1}), & i=m+1, j=1, 2, \dots, m \\ -1, & i = m+1, j=m+1. \end{cases} \quad (43)$$

525 Now, the column on the left hand side of the expression ΔN_i represents the net long wave radiation that is absorbed at each level vegetation i , as well as the soil surface layer (N_{surf}) and the atmosphere directly above the canopy (N_{above}). T_i is the temperature of each layer, and R_{LW} represents the downwelling long wave radiation from above the canopy.

Here ℓ_i represents the cumulative leaf area index when working up to level i from the ground, that is to say calculated as:

$$530 \quad \ell_i = \sum_{1}^i LAI_i \quad (44)$$

The function $\mathfrak{S}(\ell)$ simulates the effect of canopy structure on the passage of long wave radiation, and is defined as:

$$\mathfrak{S}(\ell) = 2 \int_0^1 e^{-\frac{\ell G_{leaf}(\mu)}{\mu}} \mu d\mu \quad (45)$$

$G_{leaf}(\mu)$ is a function that represents the orientation of the leaves. $\mathfrak{S}(\ell)$ is then solved from integrations.

So multiplying out the terms, we have the an expression for $\Delta\mathfrak{N}$ at each level:

$$540 \quad \Delta\mathfrak{N} = \alpha_{i,0}^{LW} \sigma(T_{surf}^t)^4 + \alpha_{i,1}^{LW} \sigma(T_{leaf,1}^t)^4 \dots, \dots + \alpha_{i,i}^{LW} \sigma(T_{leaf,i}^t)^4 \\ \dots, \dots + \alpha_{i,m}^{LW} \sigma(T_{leaf,m}^t)^4 + \alpha_{LW}^{i,m+1} R_{LW} \quad (46)$$

This part of the energy budget model is explicit, relying on temperature at the last time step. However, for the level i in each case we can make the expression semi-implicit, by expressing partly in terms of the leaf temperature at the next time step, through use a truncated Taylor expansion, such that:

$$545 \quad \alpha_{i,i}^{LW} \sigma(T_{leaf,i}^t)^4 \approx \alpha_{i,i}^{LW} \sigma(T_{leaf,i}^t)^4 + 4((T_{leaf,i}^t)^3 (T_{leaf,i}^{t+1}) - T_{leaf,i}^t) \quad (47)$$

$$\approx \alpha_{i,i}^{LW} \sigma(T_{leaf,i}^t)^3 (T_{leaf,i}^{t+1})^4 \quad (48)$$

so, in effect, Eq. (46) can be expressed as:

$$550 \quad \Delta\mathfrak{N} = \alpha_{i,0}^{LW} \sigma(T_{surf}^t)^4 + \alpha_{i,1}^{LW} \sigma(T_{leaf,1}^t)^4 \dots, \dots + \alpha_{i,i}^{LW} \sigma(T_{leaf,i}^t)^3 (T_{leaf,i}^{t+1})^4 \\ \dots, \dots + \alpha_{i,m}^{LW} \sigma(T_{leaf,m}^t)^4 + \alpha_{LW}^{i,m+1} R_{LW} \quad (49)$$

and so we calculate the matrix (44) above with the central diagonal for which $i = j$ set to zero and designate the coefficients Eq. (41) as:

$$\eta_{1,i} = \alpha_{i,i}^{LW} \sigma(T_{leaf,i}^t)^3 \quad (50)$$

555

$$\eta_{2,i} = N_i - 3\alpha_{i,i}^{LW} \sigma (T_{leaf,i}^t)^4 \quad (51)$$

3.9 The short wave radiation scheme

We implement the scheme from McGrath et al. (in prep.), which is a development of Pinty et al. (2006). The scheme accounts for three-dimensional canopies through use of a domain-averaged structure factor (the effective Leaf Area Index). To summarise, in this approach the SW radiation is divided into several terms at each level expressed as a fraction of the total SW downwelling radiation, as listed below.

Here we use the notation ψ to denote the fraction of the above canopy SW radiation that is absorbed (ψ_i^{abs}), is incoming to each level i either by direct transmission (uncollided) or by reflection (collided) (ψ_i^{in}) or is outgoing from each level i , again by collided (in either direction) or uncollided (downwards) light (ψ_i^{out}).

The symbol ' \downarrow ' refers to the sum of all downwelling shortwave radiation (i.e. directly transmitted radiation, and second order reflected radiation), whilst ' \uparrow ' refers to the sum of all upwelling shortwave radiation (i.e. sum of first-order and second-order reflected radiation from all levels).

- 570 – $\psi_{i,\downarrow}^{uncollided}$ - uncollided, transmitted albedo that represents light transmitted through level i without striking any element. This is also described as 'unscattered, collimated radiation'.
- $\psi_{i,\downarrow}^{collided}$ - collided, transmitted albedo that represents light transmitted through level i after striking vegetation one or more times. This is also described as 'forward scattered isotropic radiation'.
- 575 – $\psi_{i,\uparrow}^{collided}$ - collided, reflected albedo represents light reflected upwards after striking vegetation one or more times. This is also described as 'back scattered isotropic radiation'.

Now, using these probabilities of the fate of the light, the equations of Pinty et al. (2006) are applied to each layer of the canopy in turn, initially for the top layer, with the assumption of a black background underneath. Some of the flux is reflected back into the atmosphere, some absorbed, and some transmitted or forward scattered into the level below. The nature of the light (collimated or isotropic) determines how it interacts with the canopy, so these two types of light are accounted for separately in the model. The calculations are repeated for this lower level, with this fraction of the light. Calculations through all of the levels are continued as an iterative process until all light is accounted for through either reflection (or back scatter) back to the atmosphere or absorption by the vegetation or by the soil.

We use these terms to calculate the light that is absorbed, that is to say everything that is not either transmitted or reflected by the layer, that can be expressed as follows, respectively for the canopy top:

At the top of canopy, level 'n':

$$590 \quad \psi_{veg,n}^{abs} = 1 + \psi_{n,\uparrow,in}^{cldd} - (\psi_{n,\uparrow,out}^{cldd} + \psi_{n,\downarrow,out}^{(uncldd+cldd)}) \quad (52)$$

An intermediate level 'i':

$$\psi_i^{abs} = \psi_{i,\uparrow,in}^{cldd} + \psi_{i,\downarrow,in}^{(uncldd+cldd)} - (\psi_{i,\uparrow,out}^{cldd} + \psi_{i,\downarrow,out}^{(uncldd+cldd)}) \quad (53)$$

At vegetation level 1, where r_{bkg} is the background reflectance, at the surface layer:

$$\psi_1^{abs} = (\psi_{1,\downarrow,out}^{(uncldd+cldd)} \cdot r_{bkd}) - (\psi_{1,\uparrow,out}^{cldd} + \psi_{1,\downarrow,out}^{uncldd+cldd}) \quad (54)$$

595 So we can now say that the total canopy absorption is given by:

$$\psi_{canopy}^{abs} = \sum_{i=1}^n \psi_i^{abs} \quad (55)$$

and, making use of the above, for the soil surface layer we say:

$$\psi_{surface}^{abs} = 1 - \psi_{canopy}^{abs} - \psi_{n,\uparrow,out}^{cldd} \quad (56)$$

Over the canopy vegetation levels, we can now define the coefficient $\eta_{3,i}$ in equation Eq. (32):

$$600 \quad \eta_{3,i} = \psi_i^{abs} \quad (57)$$

$$\eta_{3,surf} = \psi_{surface}^{abs} \quad (58)$$

4 Model set up and simulations

4.1 Selected site and observations

605 Given the desired capability of the multi-layer model to simulate complex within canopy interactions, we selected a test site with an open canopy. This is because open canopies may be expected to be more complex in terms of their interactions with the overlying atmosphere. In addition, long-term data measurements of the atmospheric fluxes had to be available in order to validate the performance of the model across years and seasons, and within canopy measurements were required in order to
 610 validate the capacity of the model to simulate within canopy fluxes. One site that fulfilled these requirements was the long-term measurement site at Tumbarumba in south-eastern inland Australia (35.6°S, 148.2°E, elevation ~1200m) which is part of the global Fluxnet measurement program (Baldocchi et al., 2001). The measurement site is a *Eucalyptus Delegatensis* canopy, a temperate evergreen species, of tall height ~40m. With an LAI of ~2.4, the canopy is described as 'moderately
 615 open'. (Ozflux, 2013)

4.2 Forcing and model comparison data

As a test of stability over a long term run, the model was forced (i.e. run 'off-line', independently from the atmospheric model) using above-canopy measurements. The forcing data that was used in this simulation was derived from the long term Fluxnet measurements for the years 2002 to 2007, specifically above-canopy measurements of longwave and shortwave radiation, temperature, humidity, windspeed, rainfall and snowfall. The first four years of data, from 2002 to 2005, were used as a spin-up to charge the soil to its typical water content for the main simulation. The biomass from the spin-up was overwritten by the observed leaf biomass to impose the observed LAI profile. Soil carbon is not required in this study, which justify the short spin-up time. The years 2006 and 2007 were then used as the main part of the run. Although the shortwave radiation ~~measurements are measured in the two components, the longwave radiation measurements are~~ was recorded at the field site in upwelling and downwelling components (using a set of directional radiometers), the long wave radiation was not. As a consequence, the outgoing longwave was calculated using the recorded above canopy temperature ~~and assuming with~~ the Stefan-Boltzmann law with an emissivity factor of 0.96 (a standard technique for estimating this variable (e.g. Park et al. (2008))). This value is then subtracted from the net radiation, together with the two shortwave components, to obtain an estimation of the downwelling longwave radiation with which to force the model.

For the validation of the within canopy processes more detailed measurement data ~~was~~ were required. For the same site there exists data from an intensive campaign of measurements made during November 2006 (Austral summer), described by Haverd et al. (2009). Within the canopy, profiles of temperature and potential temperature were recorded over the 30 day period and, for a number of days (7th-14th November), sonic anemometers were used to measure windspeed and sensible heat flux in the vertical profile at eight heights as well. Measurements were also made over the thirty day period of the soil ~~heatflux~~ heat flux and the soil water content. These within-canopy data were used for validation of the modelled output but the same above-canopy long-term data (i.e. the Fluxnet data) were used in the forcing file in all cases. No further measurements were collected specifically for this publication. The measurement data (i.e. the data both from the one month intensive campaign and the long term Fluxnet measurements at the same site (Ozflux, 2013)) were prepared as an ORCHIDEE forcing file, according to the criteria for gap-filling missing data (Vuichard and Papale, 2015).

4.3 Model set-up

The multi-layer module that is described in this paper only calculates the energy budget. Its code was therefore integrated in the enhanced model ORCHIDEE-CAN, and relies on that larger model for input-output operations of drivers and simulations, as well as the calculation of soil hydrology, soil

650 heat fluxes and photosynthesis (see Table 3 for other input). A more detailed description of how these processes are implemented in ORCHIDEE-CAN is provided in [Naudts et al. \(2015\)](#) [Naudts et al. \(2014\)](#).

~~For testing the performance of the multi-layer model, rather than The ORCHIDEE-CAN, the most basic options were chosen whenever possible: (1) stomatal conductance was calculated as a function of radiation (Jarvis, 1976) rather than the default approach in ORCHIDEE-CAN that follows Ball et al. (1987) and calculates stomatal conductance as a function of net photosynthesis, relative humidity and CO_2 concentration; (2) the two-way multi-layer albedo scheme that is the default for ORCHIDEE-CAN was replaced by an exponential extinction of light as a function of LAI with increasing canopy depth; (3) although the ORCHIDEE-CAN model is capable of simulating the canopy vegetation structure dynamically, a LAD profile was prescribed in prognostically, and these prognostic vegetation stands have now been linked to the multi-layer energy budget profile in the current model. In these tests, a vegetation profile was forced, in order to obtain a simulation as close as possible to the observed conditions. That is to say, the stand height to canopy radius ratios of the trees across several size classes in ORCHIDEE-CAN were forced over the course of the spin-up phase to an approximation of the Tumbarumba LAD profile. The assigned height to radius profiles are provided in Table 4. LAD is an estimate of the sum of the surface area of all leaves growing on a given land area (e.g. per m^2) over a metre of height. It is effectively LAI (which is expressed as m^2 of leaf per unit square over an entire canopy height) recalculated per unit metre per m^2 per canopy levels, and thus has units m^2/m^3 of m^2 per level of the canopy.~~ As there were no LAD profiles available for the field site at the time of measurement, data from Lovell et al. (2012) for the ‘Tumbarumba’ profile, as depicted in Figure 3 of that publication, were used [as a template](#). The profile was scaled according to the measured site LAI of 2.4, resulting in the profile shown in Figure 2. As no gap-forming or stand ~~replacing-replacement~~ disturbances have been recorded at the site, the vertical distribution of foliage was assumed unchanged over the period between the different measurement campaigns.

675 [Several tuning coefficients were applied to constrain the model, which are listed in Table 4. A combination of manual and automated tuning was used to tune the model as closely as possible to the measurement data. The key tuning coefficients were: \$R_{b,loc}\$, a tuning coefficient for the leaf boundary layer resistance, \$R_{g,loc}\$, a coefficient for the stomatal resistance and \$R_{nf}\$, the near field correction factor to the modified eddy diffusivity coefficient \$K_i^*\$, the coefficients \$a_1\$, \$a_3\$ and \$a_5\$ corresponding to the definition \$C'_{def}\$, from Eq. \(20\) and \$\Omega\$, a correction factor for the total LAI to allow for canopy gaps. A fuller guide to the model tuning is provided in \(?\)](#).

5 Results

The sign convention used here makes all upward fluxes positive (so a positive sensible or latent heat flux from the surface cools the ground). Likewise a negative radiation flux towards the surface warms the ground.

685 Although the aim of this study is to check the performance of our multi-layer energy budget model against site-level observations, it should be noted that site-level energy fluxes come with their own limitations that result in a so-called closure gap. The closure gap is reflected in a mismatch between the net radiation and the fluxes of latent, sensible and soil heat. For the observations used in this study, the closure gap was $\sim 37 \text{ W/m}^2$ (7.5% of total fluxes) during the day and 4 W/m^2 (4.6%) during the night. ~~By design, the energy budget model conserves energy, hence, overestimates or underestimates by the model of individual fluxes by 20, which is the mean imbalance at Fluxnet sites (Wilson et al., 2002) and could be due to shortcomings in the observations.~~ Underestimation of the data and mismatches exceeding the closure gap are very likely indicate a shortcoming in the model. At a fundamental level, energy budget models distribute the net radiation between sensible, latent and soil heat fluxes. Evaluation of these component fluxes becomes only meaningful when the model reproduces the net radiation (Figure 3). Note that through its dependency on leaf temperature the calculation of the longwave component of net radiation depends on the sensible, latent and soil heat fluxes. Taken as a whole, there is a very good correlation between the observation-driven and model-driven net longwave radiation ($r^2 = 0.870.96$). However, when the data are separated into nighttime and daytime, as shown, a clear cycle is revealed, for which the model overestimates daytime radiation and underestimates radiation at night. This ~~deserepaney~~ discrepancy is likely a result of actual daytime heat storage in the soil being underestimated in the model, ~~an aspect which the model may accommodate by improved parameterisation.~~ A portion of the upwelling longwave radiation is sourced from temperature changes in fluxes from the soil model, and the rest from vegetation. So if the daytime surface layer temperature is underestimated by the model, we expect reduced net longwave predicted radiation, compared to that which is measured, and vice versa for the nighttime scenario. The use of above canopy air temperature, instead of radiative temperature (which was not measured) may also contribute to inaccuracies in the predicted longwave radiation.

705 In terms of the current parameterisation, and for the site under study, the annual cycles for both sensible and latent heat are well simulated (Figure 4a & 4(c)). In addition, no clear systematic bias was observed between summer and winter (Figure 4b & 4(d)). But, as shown, there is an overall systematic bias of $-14.8+12.7 \text{ W/m}^2$ for sensible heat and $18.5+10.7 \text{ W/m}^2$ for latent heat flux, when averaged over the whole year. Such a bias represents $\sim 2823\%$ of sensible heat and $\sim 2715\%$ of latent heat fluxes.

715 The analysis proceeded by further increasing the temporal resolution and testing the capacity of the model to reproduce diurnal flux cycles. The model overestimates the diurnal peak in sensible heat flux, whilst the latent heat flux is underestimated by a smaller magnitude (Figure 5(b)). The diurnal pattern of the model biases persists in all four seasons (Fig Supplementary 1 (a)-(d)). We

720 see that the maximum mean discrepancy between measured and modelled sensible heat flux ~~is an overestimate of roughly 90~~ ranges from +95 W/m² to -84 W/m² (Figure 5(b)) and ~~an underestimate of the~~ latent heat flux ~~by 40~~ from -49 W/m² to 43 W/m² (Figure 5(d)). Over the course of the year, the difference is largest in the autumn and smallest in the summer (Fig S2 (a)-(d)). However, from the net radiation (i.e. the sum of downwelling minus upwelling for longwave and shortwave), we can see
725 that there is a discrepancy between measured and modelled that acts to offset in part the discrepancy observed in the flux plots (Figure 5(a)-(f)). ~~This suggests that with a better parametrisation of factors within the canopy such as albedo (the impact through the shortwave radiation) and stomatal and aerodynamic resistances (which impact the partitioning between the fluxes), the model can likely be parameterised to more closely match observation.~~

730 Long-term measurements from above the forest and data from a short intensive field campaign were jointly used to evaluate model performance at different levels within the canopy. For reference, Figure S3 summarises the downwelling longwave and shortwave radiation measured over this period. As was the case for the annual cycle, the sinusoidal cycles resulting from the diurnal pattern in solar angle are well matched (Figure 6 (a)-(d)). Sensible heat flux was measured below and above the
735 canopy and the model was able to simulate this gradient (Figure 6(a), (c)). Latent heat flux at an equivalent height of 2m was not recorded (Figure 6(d)). However, the match in magnitude of the measured data is not accurately simulated hour by hour (Figure 6(e)).

Using the current parameters, there is a discrepancy between the measured and the modelled temperature gradients within the canopy (Figure 7). It should be noted that the mean values are
740 strongly determined by a few extreme hours. As such the model is capable of simulating the majority of the time steps but fails to reproduce the more extreme observations. During the daytime, the strong positive gradient in the measured output is only partly reflected in the modelled slopes. At nighttime, there is a clear negative gradient for the measured data, ~~whereas the modelled temperature profile is almost completely uniform. However a temperature profile more closely matched to the measurements (Figure ??) was achieved through forcing the eddy diffusivity coefficients by a factor (K_z) of 0.2 (nighttime) and 0.6 (daytime, as determined by the presence of SW radiation) within the canopy. The above canopy fluxes for these two simulations were however almost identical (not shown). Forcing the eddy diffusivity coefficients to better match the observations demonstrated that the observed mismatch is most likely due to the current parameterisation rather than a numerical~~
745 ~~limitation which is matched by the model. These profiles demonstrate that in-canopy gradients can be replicated by parameterisation~~ of the model.

The version of the model used in these tests so far is composed of 50 levels, 30 levels, with 10 levels in the understorey, 10 in the canopy vegetation profile, and 10 in the overstorey, in order to provide a high resolution simulation and a test of the stability of the scheme. However, a canopy
755 simulation of such detail is likely might be overly complex for a canopy model that is to be coupled to an atmospheric simulation, in terms of additional run time required, ~~and is probably unnecessary~~. To

provide an evaluation of the difference in fluxes that were predicted by a model of lower resolution, the same tests were conducted with the model composed of 25, 10, 5, 2 and a single vegetation level, that correspond to a profile that totals 30, 15, 8 and 5 levels over all, when the levels in the overstorey and understorey are included (note that in all cases the vegetation levels are simulated separately from the surface soil, so the single vegetation model is a two-layer canopy model in the sense that the two levels are the canopy and the soil level is also treated separately in each case, and represents a separate layer (c.f., Dolman, 1993)). When taken in the context of the annual simulations for-

765 Tests were conducted for both hourly mean (Figure 8) and daily mean (Figure 9), both calculated over the course of a year, and for a moving average. These plots show the 50-layer case (Figure 5); these tests show that the difference is slight between the 50-layer and 25-layer case, and between the 50-layer and 10-layer case for both sensible and latent heat (Figure 8). In all cases the mean hourly difference over the whole year is always less than RMS error between the original set up and the modified number of levels. Looking first at the plots for hourly mean, we see that there is already a significant difference between the calculated sensible heat flux for the version of the model with 10 canopy layers (30 total profile layers) and 5 W/m^2 per flux (~ 3 of the 50 level mean). For the two-vegetation layer model the mean hourly difference is always less than 20 canopy layers (15 total profile layers), that reaches a peak of 28 W/m^2 per flux (~ 10 approx.) and for the one-layer vegetation model (with the soil surface modelled separately), the mean hourly difference is always less than 55, but that the discrepancy is substantially larger for the 2 canopy layer (8 total levels) and a single canopy layer (5 total levels) cases. In the case of the latent heat flux, the discrepancy is most marked for the the single canopy layer case, with a peak difference of 60 W/m^2 per flux (~ 30 approx.). Figure 9 presents the average RMS error for each day of the year (shown as a rolling average). Considering the daily averages, for sensible heat flux the difference between the different model set-ups is always below 25 W/m^2 in all cases. For latent heat flux, there is more considerable divergence, up to 42 W/m^2 , for the single canopy later set-up.

6 Discussion

The proposed model is able to simulate fluxes of sensible and latent heat above the canopy over a long term period, as has been shown by simulation of conditions at a Fluxnet site on a long term, annual scale (Figures 4 and 5), and over a concentrated, week-long period (Figure 6). Although these figures show a discrepancy between measured and modelled fluxes, we see from Figure 5 that the modelled overestimate of sensible heat flux is offset by an underestimation of latent heat flux and of net radiation. It is likely therefore that this discrepancy can be reduced by an improved simulation of canopy albedo at each level (which determines the distribution and reflection of shortwave radiation over the modelled canopy), and refinements to the calculation of vegetation aerodynamic and stomatal

~~resistances (which affects the split between sensible and latent heat from each modelled layer).~~ In the study of land-atmosphere interactions, the multi-layer model functions to a standard comparable to single-layer models, and an interactive model applied to the same site (Haverd et al., 2009) found differences of the order of 50 W/m^2 at maximum for the mean daily average latent and sensible above canopy heat fluxes.

The innovation of this model is the capacity to simulate the behaviour of fluxes within the canopy, and the separation of the soil-level temperature from the temperature of the vegetation levels. Uniquely for a canopy model, this is achieved without iterations, as the mathematics have been derived to use the same implicit coupling technique as the existing surface-atmosphere coupling applied in ORCHIDEE/LMDz (Polcher et al., 1998; Best et al., 2004), but now over the height of the canopy. This also means that the model is scalable without impacting heavily on runtimes. For large scale applications, performance within the canopy must be further constrained through comparison with intensive in-canopy field campaigns from diverse ecosystems.

6.1 Simulation of aerodynamic resistance

In this study, the aerodynamic coefficient that is used in single-layer models was replaced by an eddy diffusivity profile, the purpose of which is two-fold. Firstly, to develop a transport coefficient that is based on the vertical canopy profile and secondly, to more accurately represent the in-canopy gradients of temperature and specific humidity. In this way, it was hoped to contribute to a model that can better allow for such features as vertical canopy gaps (i.e. trunk space between a well separated under and overstorey), horizontal gaps, transport and chemistry between different sections of the canopy, tree growth and the mix of different kinds of vegetation in the same surface layer simulation (e.g. Dolman (1993)). To be able to do this, a height based transport closure model was used to simulate within canopy transport.

~~A~~ The transport closure model contrasts the existing used here can be compared to the previous single-layer approach within ORCHIDEE, as is used in single layer models. In that approach, aerodynamic interaction between the land surface and the atmosphere is parametrised by the atmospheric resistance R_a and the architectural resistance R_0 . R_a is typically calculated through consideration of the roughness height of the canopy (i.e. small for flat surfaces, large for uneven tall surfaces) which in turn is parameterised in surface layer models by canopy height (e.g., LSCE/IPSL, 2012) (however, LAI can display a better correlation with roughness length (a critical parameter) than it does to canopy height (Beringer et al., 2005)). In parameterising the roughness length in terms of canopy height alone, no account is made for the clumping of trees, the density of the forest or the phenological changes in stand profile (other than the height) as the stand grows. Some of these changes are compensated for in R_0 , the structural coefficient that is unique to each PFT grouping, but does not allow for more subtle effects. To be able to satisfactorily explore such results in a modelling study requires an accurate parametrisation of within-canopy transport.

In this study, canopy transport is parametrised by K-theory, applying the closure model of Massman and Weil (1999) to derive the in-canopy turbulence statistics, based both on the LAI profile and the canopy height. The simulation produces a good estimation of above-canopy fluxes, but the differences between day- and night- time profiles are not well described using the original parametrisation (Figure 7). This means that the model overestimates the nighttime canopy transport, as compared to the daytime simulation.

Looking more broadly, studies of chemical species transport have demonstrated that K-theory, sometimes constrained by a scaling factor, remains a reasonable approximation for above-canopy fluxes, even if the within-canopy gradients are not entirely correct (Gao et al., 1989; Dolman and Wallace, 1991; Makar et al., 1999; Wolfe and Thornton, 2010). The justification for such a scaling factor seems to vary in terms of the form of the canopy structure, likely related to canopy openness (McNaughton and van den Hurk, 1995; Stroud et al., 2005). Here, too, we find that a scaling factor is necessary to match the gradient fluxes though the scaling factor required varies according to the time of day. ~~During the nighttime (Figures ??(a) and ??(d)), the measurements show a general positive temperature gradient (as defined from the soil surface moving upwards), which could be replicated through the use of an eddy coefficient factor of 0.2. During the daytime (Figures ??(b) and ??(e)), the negative gradient can be replicated most closely with an eddy coefficient factor of 0.6. Parametrisation of models, against the growing amount of detailed canopy measurement campaigns will help to clarify the issue.~~ We now also parameterise the effective phytoelement canopy drag coefficient, C_{Defl} , in order to obtain a more accurate simulation. For a completely satisfactory resolution of this issue, it will be necessary to derive a method to reformulate the method of Raupach (1989a, b) in an implicit form, which lies outside the realm scope of this paper.

6.2 Simulation of energy partition throughout canopy and soil surface

Trees in a spruce forest have been reported to account for 50% - 60% of the latent heat flux; moisture in the soil itself would have a reduced impact due to soil shading (Baldocchi et al., 2000). Another study found that the fraction of radiation that reaches the soil ranges from 0.05 (forest) to 0.12 (tundra) (Beringer et al., 2005). The same study found that the latent heat flux correlates most closely with the leaf-level vapour pressure deficit - that is to say the difference between the leaf level saturation vapour pressure and the actual vapour pressure of the outside air, rather than between air water vapour pressure and the saturation vapour pressure at the soil level. Since a single layer canopy model regards both the canopy and soil surface as the same entity, the aforementioned subtleties will inevitably be lost in the modelling. Although, the partition of energy between soil surface and vegetation is site dependent - a well hydrated site would behave differently to one in an arid region - it is effects such as these that a more realistic energy budget scheme would be able to simulate.

Being able to simulate separately the vegetation allows for the partitioning of fluxes between the vegetation and the soil. For example, from the measurements (Figure ??-6 (a) and (b)), we see that

approximately 50% of the sensible heat that is measured above the canopy is sourced not from the
865 soil surface, but from the overlying vegetation, as this is the difference between the measured flux
at 1m and that above the canopy. ~~This is confirmed by the modelling results~~ The modelling results
here overestimate the measured contribution from the soil. There is no equivalent measurement at
1m for the latent heat flux, but the model calculates that approximately 50% of the latent heat flux is
sourced from the vegetation rather than the soil surface.

870 This model also simulates leaf temperature that may be verified by leaf level measurements, where
such measurements exist (Helliker and Richter, 2008). Such a comparison would require additional
developments (as is discussed in the following section) because leaf temperature measurements
strongly depend on the approach that is used.

7 Outlook

875 This document lays out the framework for the model design, but it allows for the further implemen-
tation of many features in site-level to global-scale scenarios:

- As the method calculates leaf temperature and in-canopy radiation, it will be possible to simu-
late the explicit emission by leaves of certain common Biogenic Volatile Organic Compounds
(BVOCs), such as isoprene and monoterpene (Guenther et al., 1995, 2006). As the method
880 calculates in-canopy gradients of temperature, specific humidity and radiation, it is possi-
ble to simulate more accurately chemical reactions that depend on these factors such as the
 NO_x and O_3 cycle within and above canopies (Walton et al., 1997) and the formation and
size distribution of aerosol interactions (Atkinson and Arey, 2003; Nemitz et al., 2004a, b;
Ehn et al., 2014), which may act as cloud condensation nuclei and thus again feedback into
885 radiation absorption interactions at the atmospheric component of a coupled model such as
LMDz/ORCHIDEE.
- Separate computation of vegetation and soil temperatures, which can be very different, and
then to estimate accurate estimation of the whole canopy temperature and its directional ef-
fects. It may then be possible to assimilate this variable (which can also be measured from
890 remote sensing) in order to better constrain the energy budget.
- Recent research in ecology demonstrates further the need to better understand canopy mi-
croclimates, and in particular gradients of state variables such as temperature and specific
humidity, and radiation penetration. For example, temperature gradients in the rainforest exert
a key influence on the habitat choices of frogs, and changes to such a microclimate threaten
895 their survival (Scheffers et al., 2013). In a similar vein, microclimate affects in canopies can
act as a buffer to changes in the climate overall (i.e. the ~~macroclimate~~ macro-climate) in terms
of the survival of species in the sub-canopy (Defraeye et al., 2014). Therefore structural forest

changes, such as forest thinning, will reduce buffer lag effect, but it is only with well-designed canopy models that an informed prediction of the long term consequences of land management policies can be made.

8 Conclusions

A new numerical model for ORCHIDEE-CAN has been developed that enables the simulation of vertical canopy profiles of temperature and moisture using a non-iterative implicit scheme. This means that the new model may also be used when coupled to an atmospheric model, without compromising computer run-time. Initial tests demonstrated that the model runs stably, balances the energy budget at all levels, and provides a good simulation of the measured field data, both on short timescales of a few days, and over the course of a year. ~~However~~ As demonstrated, the model structure allows coupling/linking to a more physical-based albedo scheme (Pinty et al., 2006; McGrath et al., in prep.; Naudts et al., 2015) and implementing (Pinty et al., 2006; McGrath et al., in prep.; Naudts et al., 2014) and the implementation of a vertically discretised stomatal conductance scheme ~~which both offer scope for improvement in model performance~~. Reducing the vertical discretisation of the canopy from 10 layers to 5, 2 and 1 layer increased the RMSE between the model and the observations for LE and H and thus demonstrates the overall benefits of introducing a multi-layer energy budget scheme. The multi-layer energy budget model component outlined here may be used to simulate canopies in more detail and variety.. It also offers the potential to integrate with other parts of ORCHIDEE for enhanced simulation of CO_2 transport, emission of VOCs and leaf scale plant hydraulics.

9 Author Contributions

JR and JP developed the numerical scheme. ~~JR~~ YC and JR developed the parameterisation scheme. JR, JP, CO, PP and SL designed the study and JR and SL wrote the manuscript with contributions from all co-authors. YC, MJM, JO, KN, SL and AV helped JR with integrating the multi-layer energy budget model within ORCHIDEE-CAN. EvG and VH provided field observations for the Tumbarumba site.

Acknowledgements. JR, YC, MJM, JO, KN and SL were funded through ERC starting grant 242564 (DO-FOCO), and AV was funded through ADEME (BiCaFF). ESA CCI Landcover also supported this work. The study benefited from an STSM (COST, TERRABITES ES0805) offered to JR. We thank the three anonymous reviewers for their very helpful observations and suggestions. The authors would like to thank Aaron Boone for sharing his numerical scheme of an implicit coupling of snowpack and atmosphere temperature. Plots were produced using matplotlib software (Hunter, 2007).

References

- 930 Atkinson, R. and Arey, J.: Gas-phase tropospheric chemistry of biogenic volatile organic compounds: a review, *Atmospheric Environment*, 37, 197–219, doi:10.1016/S1352-2310(03)00391-1, <http://linkinghub.elsevier.com/retrieve/pii/S1352231003003911>, 2003.
- Baldocchi, D. D.: A multi-layer model for estimating sulfur dioxide deposition to a deciduous oak forest canopy, *Atmospheric Environment* (1967), 22, 869–884, doi:10.1016/0004-6981(88)90264-8, <http://linkinghub.elsevier.com/retrieve/pii/0004698188902648>, 1988.
- 935 Baldocchi, D. D. and Wilson, K.: Modeling CO₂ and water vapor exchange of a temperate broadleaved forest across hourly to decadal time scales, *Ecological Modelling*, 142, 155–184, doi:10.1016/S0304-3800(01)00287-3, <http://www.sciencedirect.com/science/article/pii/S0304380001002873>, 2001.
- Baldocchi, D. D., Law, B. E., and Anthoni, P. M.: On measuring and modeling energy fluxes above the floor of a homogeneous and heterogeneous conifer forest, *Agricultural and Forest Meteorology*, 102, 187–206, doi:10.1016/S0168-1923(00)00098-8, <http://linkinghub.elsevier.com/retrieve/pii/S0168192300000988>, 2000.
- 940 Baldocchi, D. D., Falge, E., Gu, L., Olson, R., Hollinger, D. Y., Running, S., Anthoni, P., Bernhofer, C., Davis, K., and Evans, R.: FLUXNET: A new tool to study the temporal and spatial variability of ecosystem-scale carbon dioxide, water vapor, and energy flux densities., *Bulletin of the American Meteorological Society*, 82, 2415–2434, <http://ddr.nal.usda.gov/handle/10113/118>, 2001.
- Ball, J. T., Woodrow, T., and Berry, J.: A model predicting stomatal conductance and its contribution to the control of photosynthesis under different environmental conditions, in: *Proceedings of the 7th International Congress on Photosynthesis*, pp. 221–224, 1987.
- 950 Balsamo, G., Beljaars, A., Scipal, K., Viterbo, P., van den Hurk, B., Hirschi, M., and Betts, A. K.: A revised hydrology for the ECMWF model: verification from field site to terrestrial water storage and impact in the integrated forecast system, *Journal of Hydrometeorology*, 10, 623–643, doi:10.1175/2008JHM1068.1, <http://journals.ametsoc.org/doi/abs/10.1175/2008JHM1068.1>, 2009.
- Beringer, J., Chapin, F. S., Thompson, C. C., and Mcguire, A. D.: Surface energy exchanges along a tundra-forest transition and feedbacks to climate, *Agricultural and Forest Meteorology*, 131, 143–161, doi:10.1016/j.agrformet.2005.05.006, 2005.
- 955 Best, M. J., Beljaars, A. C. M., Polcher, J., and Viterbo, P.: A proposed structure for coupling tiled surfaces with the planetary boundary layer, *Journal of Hydrometeorology*, 5, 1271–1278, 2004.
- Bonan, G. B.: Forests and climate change: forcings, feedbacks, and the climate benefits of forests, *Science*, 320, 1444–1449, doi:10.1126/science.1155121, <http://www.sciencemag.org/content/320/5882/1444.short>, 2008.
- 960 Bonan, G. B., Williams, M., Fisher, R. a., and Oleson, K. W.: Modeling stomatal conductance in the earth system: linking leaf water-use efficiency and water transport along the soil–plant–atmosphere continuum, *Geoscientific Model Development*, 7, 2193–2222, doi:10.5194/gmd-7-2193-2014, <http://www.geosci-model-dev.net/7/2193/2014/>, 2014.
- 965 Chen, J., Menges, C., and Leblanc, S.: Global mapping of foliage clumping index using multi-angular satellite data, *Remote Sensing of Environment*, 97, 447–457, doi:10.1016/j.rse.2005.05.003, <http://linkinghub.elsevier.com/retrieve/pii/S0034425705001550>, 2005.

- de Noblet-Ducoudré, N., Boisier, J.-P., Pitman, A., Bonan, G. B., Brovkin, V., Cruz, F., Delire, C., Gayler, V., van den Hurk, B. J. J. M., Lawrence, P. J., van der Molen, M. K., Müller, C., Reick, C. H., Strengers, B. J., and Voldoire, A.: Determining robust impacts of land-use-induced land cover changes on surface climate over North America and Eurasia: Results from the first set of LUCID experiments, *Journal of Climate*, 25, 3261–3281, doi:10.1175/JCLI-D-11-00338.1, <http://journals.ametsoc.org/doi/abs/10.1175/JCLI-D-11-00338.1>, 2012.
- Defraeye, T., Derome, D., Verboven, P., Carmeliet, J., and Nicolai, B.: Cross-scale modelling of transpiration from stomata via the leaf boundary layer, *Annals of Botany*, 114, 711–723, doi:10.1093/aob/mct313, <http://www.ncbi.nlm.nih.gov/pubmed/24510217>, 2014.
- Dobos, E.: Albedo, in: *Encyclopedia of Soil Science*, 2nd Edition, edited by Lal, R., CRC Press, doi:10.1201/NOE0849338304.ch15, 2005.
- Dolman, A. J.: A multiple-source land surface energy balance model for use in general circulation models, *Agricultural and Forest Meteorology*, 65, 21–45, doi:10.1016/0168-1923(93)90036-H, <http://linkinghub.elsevier.com/retrieve/pii/016819239390036H>, 1993.
- Dolman, A. J. and Wallace, J.: Lagrangian and K-theory approaches in modelling evaporation from sparse canopies, *Quarterly Journal of the Royal Meteorological Society*, 117, 1325–1340, <http://onlinelibrary.wiley.com/doi/10.1002/qj.49711750210/abstract>, 1991.
- Ehn, M., Thornton, J. A., Kleist, E., Sipilä, M., Junninen, H., Pullinen, I., Springer, M., Rubach, F., Tillmann, R., Lee, B., Lopez-Hilfiker, F., Andres, S., Acir, I.-H., Rissanen, M., Jokinen, T., Schobesberger, S., Kangasluoma, J., Kontkanen, J., Nieminen, T., Kurtén, T., Nielsen, L. B., Jørgensen, S., Kjaergaard, H. G., Canagaratna, M., Maso, M. D., Berndt, T., Petäjä, T., Wahner, A., Kerminen, V.-M., Kulmala, M., Worsnop, D. R., Wildt, J., and Mentel, T. F.: A large source of low-volatility secondary organic aerosol, *Nature*, 506, 476–9, doi:10.1038/nature13032, <http://www.ncbi.nlm.nih.gov/pubmed/24572423>, 2014.
- Gao, W., Shaw, R. H., and Paw, K. T.: Observation of organized structure in turbulent flow within and above a forest canopy, *Boundary-Layer Meteorology*, 47, 349–377, 1989.
- Gu, L.: Longwave radiative transfer in plant canopies, Ph.D. thesis, University of Virginia, 1988.
- Gu, L., Shugart, H. H., Fuentes, J. D., Black, T. A., and Shewchuk, S. R.: Micrometeorology, biophysical exchanges and NEE decomposition in a two-storey boreal forest - development and test of an integrated model, *Agricultural and Forest Meteorology*, 94, 123–148, 1999.
- Guenther, A., Karl, T., Harley, P., Wiedinmyer, C., Palmer, P. I., and Geron, C.: Estimates of global terrestrial isoprene emissions using MEGAN (Model of Emissions of Gases and Aerosols from Nature), *Atmospheric Chemistry and Physics Discussions*, 6, 107–173, doi:10.5194/acpd-6-107-2006, <http://www.atmos-chem-phys-discuss.net/6/107/2006/>, 2006.
- Guenther, A. B., Nicholas, C., Fall, R., Klinger, L., McKay, W. A., and Scholes, B.: A global model of natural volatile organic compound emissions, *Journal of Geophysical Research*, 100, 8873–8892, 1995.
- Haverd, V., Leuning, R., Griffith, D., Gorsel, E., and Cuntz, M.: The turbulent Lagrangian time scale in forest canopies constrained by fluxes, concentrations and source distributions, *Boundary-Layer Meteorology*, 130, 209–228, doi:10.1007/s10546-008-9344-4, <http://www.springerlink.com/index/10.1007/s10546-008-9344-4>, 2009.

- Helliker, B. R. and Richter, S. L.: Subtropical to boreal convergence of tree-leaf temperatures, *Nature*, 454, 511–4, doi:10.1038/nature07031, <http://www.ncbi.nlm.nih.gov/pubmed/18548005>, 2008.
- Hourdin, F.: Etude et simulation numérique de la circulation générale des atmosphères planétaires, Ph.D. thesis, 1010 1992.
- Hourdin, F., Musat, I., Bony, S., Braconnot, P., Codron, F., Dufresne, J.-L., Fairhead, L., Filiberti, M.-A., Friedlingstein, P., Grandpeix, J.-Y., Krinner, G., LeVan, P., Li, Z.-X., and Lott, F.: The LMDZ4 general circulation model: climate performance and sensitivity to parametrized physics with emphasis on tropical convection, *Climate Dynamics*, 27, 787–813, doi:10.1007/s00382-006-0158-0, <http://www.springerlink.com/index/10.1007/s00382-006-0158-0>, 2006.
- Hunter, J. D.: Matplotlib: A 2D graphics environment, *Computing In Science & Engineering*, 9, 90–95, 2007.
- Jarvis, P.: The interpretation of the variations in leaf water potential and stomatal conductance found in canopies in the fields, *Philosophical Transactions of the Royal Society of London, Series B*, pp. 593–610, 1976.
- Jiménez, C., Prigent, C., Mueller, B., Seneviratne, S. I., McCabe, M. F., Wood, E. F., Rossow, W. B., Balsamo, 1020 G., Betts, A. K., Dirmeyer, P. A., Fisher, J. B., Jung, M., Kanamitsu, M., Reichle, R. H., Reichstein, M., Rodell, M., Sheffield, J., Tu, K., and Wang, K.: Global intercomparison of 12 land surface heat flux estimates, *Journal of Geophysical Research*, 116, D02 102, doi:10.1029/2010JD014545, <http://doi.wiley.com/10.1029/2010JD014545>, 2011.
- Krinner, G., Viovy, N., de Noblet-Ducoudré, N., Ogee, J., Polcher, J., Friedlingstein, P., Ciais, P., Sitch, S., and 1025 Prentice, I. C.: A dynamic global vegetation model for studies of the coupled atmosphere-biosphere system, *Global Biogeochemical Cycles*, 19, 1–33, doi:10.1029/2003GB002199, 2005.
- Lohammer, T., Larsson, S., Linder, S., and Falk, S. O.: Simulation models of gaseous exchange in Scotch pine. Structure and function of Northern Coniferous Forest, *Ecological Bulletin*, 32, 505–523, 1980.
- Lovell, J., Haverd, V., Jupp, D., and Newnham, G.: The Canopy Semi-analytic Pgap And Radiative Transfer (CanSPART) model: Validation using ground based lidar, *Agricultural and Forest Meteorology*, 158-159, 1–12, doi:10.1016/j.agrformet.2012.01.020, <http://linkinghub.elsevier.com/retrieve/pii/S0168192312000512>, 2012.
- LSCE/IPSL: ORCHIDEE documentation (as at forge.ipsl.jussieu.fr/orchidee/wiki/Documentation), 2012.
- Makar, P. A., Fuentes, J. D., Wang, D., Staebler, R. M., and Wiebe, H. A.: Chemical processing of biogenic 1035 hydrocarbons within and above a temperate deciduous forest, *Journal of Geophysical Research*, 104, 3581–3603, doi:10.1029/1998JD100065, <http://www.agu.org/pubs/crossref/1999/1998JD100065.shtml>, 1999.
- Martens, S. N., Ustin, S. L., and Rousseau, R. A.: Estimation of tree canopy leaf area index by gap fraction analysis, *Forest Ecology and Management*, 61, 91–108, 1993.
- Massman, W. J. and Weil, J. C.: An analytical one-dimensional second-order closure model of turbulence statistics and the lagrangian time scale within and above plant canopies of arbitrary structure, *Boundary-Layer Meteorology*, 91, 81–107, 1999.
- McGrath, M. J., Pinty, B., Ryder, J., Otto, J., and Luysaert, S.: A multilevel canopy radiative transfer scheme based on a domain-averaged structure factor, in prep.
- McNaughton, K. G. and van den Hurk, B. J. J. M.: A 'Lagrangian' revision of the resistors in the two-layer 1045 model for calculating the energy budget of a plant canopy, *Boundary-Layer Meteorology*, 74, 261–288, 1995.

- Medlyn, B. E., Duursma, R. A., Eamus, D., Ellsworth, D. S., Prentice, I. C., Barton, C. V. M., Crous, K. Y., De Angelis, P., Freeman, M., and Wingate, L.: Reconciling the optimal and empirical approaches to modelling stomatal conductance, *Global Change Biology*, 17, 2134–2144, doi:10.1111/j.1365-2486.2010.02375.x, <http://doi.wiley.com/10.1111/j.1365-2486.2010.02375.x>, 2011.
- 1050
- Monteith, J. and Unsworth, M. H.: *Principles of Environmental Physics*, Elsevier, 2008.
- Naudts, K., Ryder, J., J. McGrath, M., Otto, J., Chen, Y., Valade, a., Bellasen, V., Berhongaray, G., Bönisch, G., Campioli, M., Ghattas, J., De Groote, T., Haverd, V., Kattge, J., MacBean, N., Maignan, F., Merilä, P., Penuelas, J., Peylin, P., Pinty, B., Pretzsch, H., Schulze, E. D., Solyga, D., Vuichard, N., Yan, Y., and
- 1055
- Luyssaert, S.: A vertically discretised canopy description for ORCHIDEE (SVN r2290) and the modifications to the energy, water and carbon fluxes, *Geoscientific Model Development Discussions*, 7, 8565–8647, doi:10.5194/gmdd-7-8565-2014, 2014.
- Naudts, K., Ryder, J., McGrath, M. J., Otto, J., Chen, Y., Valade, a., Bellasen, V., Berhongaray, G., Bönisch, G., Campioli, M., Ghattas, J., De Groote, T., Haverd, V., Kattge, J., MacBean, N., Maignan, F., Merilä,
- 1060
- P., Penuelas, J., Peylin, P., Pinty, B., Pretzsch, H., Schulze, E. D., Solyga, D., Vuichard, N., Yan, Y., and Luyssaert, S.: A vertically discretised canopy description for ORCHIDEE (SVN r2290) and the modifications to the energy, water and carbon fluxes, *Geoscientific Model Development*, 8, 2035–2065, doi:10.5194/gmd-8-2035-2015, <http://www.geosci-model-dev.net/8/2035/2015/>, 2015.
- Nemitz, E. G., Sutton, M. A., Wyers, G. P., and Jongejan, P. A. C.: Gas-particle interactions above a Dutch
- 1065
- heathland: I. Surface exchange fluxes of NH₃, SO₂, HNO₃ and HCl, *Atmospheric Chemistry and Physics*, 4, 989–1005, 2004a.
- Nemitz, E. G., Sutton, M. A., Wyers, G. P., Otjes, R. P., Mennen, M. G., Putten, E. M. V., and Gallagher, M. W.: Gas-particle interactions above a Dutch heathland: II. Concentrations and surface exchange fluxes of atmospheric particles, *Atmospheric Chemistry and Physics*, 4, 1007–1024, 2004b.
- 1070
- Nobel, P. S.: *Physiochemical and environmental plant physiology*, Elsevier, 3 edn., 0-12-520026-9, 2005.
- Ogé, J., Brunet, Y., Loustau, D., Berbigier, P., and Delzon, S.: MuSICA, a CO₂, water and energy multi-layer, multileaf pine forest model: evaluation from hourly to yearly time scales and sensitivity analysis, *Global Change Biology*, 9, 697–717, doi:10.1046/j.1365-2486.2003.00628.x, <http://doi.wiley.com/10.1046/j.1365-2486.2003.00628.x>, 2003.
- 1075
- Ozflux: Description of Tumbarumba monitoring station (as at www.ozflux.org.au/monitoringsites/tumbarumba), www.ozflux.org.au/monitoringsites/tumbarumba, 2013.
- Park, G.-H., Gao, X., and Sorooshian, S.: Estimation of surface longwave radiation components from ground-based historical net radiation and weather data, *Journal of Geophysical Research*, 113, D04 207, doi:10.1029/2007JD008903, <http://doi.wiley.com/10.1029/2007JD008903>, 2008.
- 1080
- Penman, H. L. and Schofield, R. K.: Some physical aspects of assimilation and transpiration, *Symp. Soc. Exp. Biol.*, 5, 115–129, 1951.
- Pinty, B., Lavergne, T., Dickinson, R. E., Widlowski, J.-L., Gobron, N., and Verstraete, M. M.: Simplifying the interaction of land surfaces with radiation for relating remote sensing products to climate models, *Journal of Geophysical Research*, 111, 1–20, doi:10.1029/2005JD005952, <http://www.agu.org/pubs/crossref/2006/2005JD005952.shtml>, 2006.
- 1085

- Pitman, A. J., de Noblet-Ducoudré, N., Cruz, F. T., Davin, E. L., Bonan, G. B., Brovkin, V., Claussen, M., Delire, C., Ganzeveld, L., Gayler, V., van den Hurk, B. J. J. M., Lawrence, P. J., van der Molen, M. K., Müller, C., Reick, C. H., Seneviratne, S. I., Strengers, B. J., and Voldoire, A.: Uncertainties in climate responses to past land cover change: First results from the LUCID intercomparison study, *Geophysical Research Letters*, 36, L14 814, doi:10.1029/2009GL039076, <http://www.agu.org/pubs/crossref/2009/2009GL039076.shtml>, 2009.
- 1090 Polcher, J., McAvaney, B., Viterbo, P., Gaertner, M., Hahmann, A., Mahfouf, J.-F., Noilhan, J., Phillips, T., Pitman, A. J., Schlosser, C., Schulz, J.-P., Timbal, B., Verseghy, D. L., and Xue, Y.: A proposal for a general interface between land surface schemes and general circulation models, *Global and Planetary Change*, 19, 261–276, <http://www.sciencedirect.com/science/article/pii/S0921818198000526>, 1998.
- 1095 Press, W. H.: *Numerical recipes in Fortran 77: Second edition*, Cambridge University Press, 1992.
- Raupach, M. R.: Applying Lagrangian fluid mechanics to infer scalar source distributions from concentration profiles in plant canopies, *Agricultural and Forest Meteorology*, 47, 85–108, 1989a.
- Raupach, M. R.: A practical Lagrangian method for relating scalar concentrations to source distributions in vegetation canopies, *Quarterly Journal of the Royal Meteorological Society*, 115, 609–632, doi:10.1256/smsqj.48709, <http://www.ingentaselect.com/rpsv/cgi-bin/cgi?ini=xref&body=linker&reqdoi=10.1256/smsqj.48709>, 1989b.
- 1100 Richtmyer, R. D. and Morton, K. W.: *Difference Methods for Initial-Value Problems* (second edition), Wiley-Interscience, 1967.
- Saux-Picart, S., Ottlé, C., Perrier, a., Decharme, B., Coudert, B., Zribi, M., Boulain, N., Cappelaere, B., and 1105 Ramier, D.: SEtHyS_Savannah: A multiple source land surface model applied to Sahelian landscapes, *Agricultural and Forest Meteorology*, 149, 1421–1432, doi:10.1016/j.agrformet.2009.03.013, <http://linkinghub.elsevier.com/retrieve/pii/S0168192309000847>, 2009.
- Scheffers, B. R., Phillips, B. L., Laurance, W. F., Sodhi, N. S., Diesmos, A., Williams, E., and Williams, S. E.: Increasing arboreality with altitude: a novel biogeographic dimension, *Proceedings of the The Royal Society B*, 280, 1–9, doi:10.1098/rspb.2013.1581, 2013.
- 1110 Schlosser, C. A. and Gao, X.: Assessing Evapotranspiration Estimates from the Second Global Soil Wetness Project (GSWP-2) Simulations, *Journal of Hydrometeorology*, 11, 880–897, doi:10.1175/2010JHM1203.1, <http://journals.ametsoc.org/doi/abs/10.1175/2010JHM1203.1>, 2010.
- Schulz, J.-P., Dümenil, L., and Polcher, J.: On the Land Surface–Atmosphere Coupling and Its 1115 Impact in a Single-Column Atmospheric Model, *Journal of Applied Meteorology*, 40, 642–663, doi:10.1175/1520-0450(2001)040<0642:OTLSAC>2.0.CO;2, [http://journals.ametsoc.org/doi/abs/10.1175/1520-0450\(2001\)040<0642:OTLSAC>2.0.CO;2](http://journals.ametsoc.org/doi/abs/10.1175/1520-0450(2001)040<0642:OTLSAC>2.0.CO;2), 2001.
- Seneviratne, S. I., Corti, T., Davin, E. L., Hirschi, M., Jaeger, E. B., Lehner, I., Orlowsky, B., and Teuling, A. J.: Investigating soil moisture–climate interactions in a changing climate: A review, *Earth-Science Reviews*, 99, 125–161, doi:10.1016/j.earscirev.2010.02.004, <http://linkinghub.elsevier.com/retrieve/pii/S0012825210000139>, 2010.
- 1120 Shuttleworth, W. J. and Wallace, J. S.: Evaporation from sparse crops - an energy combination theory, *Quarterly Journal of the Royal Meteorological Society*, 111, 839–855, doi:10.1256/smsqj.46909, <http://www.ingentaselect.com/rpsv/cgi-bin/cgi?ini=xref&body=linker&reqdoi=10.1256/smsqj.46909>, 1985.

- 1125 Singles, R., Sutton, M., and Weston, K.: A multi-layer model to describe the atmospheric transport and deposition of ammonia in Great Britain, *Atmospheric Environment*, 32, 393–399, doi:10.1016/S1352-2310(97)83467-X, <http://linkinghub.elsevier.com/retrieve/pii/S135223109783467X>, 1998.
- Sinoquet, H., Le Roux, X., Adam, B., Ameglio, T., and Daudet, F. A.: RATP: a model for simulating the spatial distribution of radiation absorption, transpiration and photosynthesis within canopies: application to an isolated tree crown, *Plant, Cell and Environment*, 24, 395–406, doi:10.1046/j.1365-3040.2001.00694.x, <http://doi.wiley.com/10.1046/j.1365-3040.2001.00694.x>, 2001.
- 1130 Stroud, C., Makar, P. A., Karl, T., Guenther, A. B., Geron, C., Turnipseed, A., Nemitz, E. G., Baker, B., Potosnak, M. J., and Fuentes, J. D.: Role of canopy-scale photochemistry in modifying biogenic-atmosphere exchange of reactive terpene species: Results from the CELTIC field study, *Journal of Geophysical Research*, 110, 1–14, doi:10.1029/2005JD005775, <http://www.agu.org/pubs/crossref/2005/2005JD005775.shtml>, 2005.
- Verhoef, A. and Allen, S. J.: A SVAT scheme describing energy and CO₂ fluxes for multi-component vegetation: calibration and test for a Sahelian savannah, *Ecological Modelling*, 127, 245–267, doi:10.1016/S0304-3800(99)00213-6, <http://linkinghub.elsevier.com/retrieve/pii/S0304380099002136>, 2000.
- 1140 Vieno, M.: The use of an atmospheric chemistry-transport model (FRAME) over the UK and the development of its numerical and physical schemes, Ph.D. thesis, University of Edinburgh, 2006.
- Vuichard, N. and Papale, D.: Filling the gaps in meteorological continuous data measured at FLUXNET sites with ERA-interim reanalysis, *Earth System Science Data Discussions*, 8, 23–55, doi:10.5194/essdd-8-23-2015, www.earth-syst-sci-data-discuss.net/8/23/2015/, 2015.
- 1145 Waggoner, P. E., Furnival, G. M., and Reifsnyder, W. E.: Simulation of the microclimate in a forest, *Forest Science*, 15, 37–45, 1969.
- Walton, S., Gallagher, M. W., and Duyzer, J. H.: Use of a detailed model to study the exchange of NO_x and O₃ above and below a deciduous canopy, *Atmospheric Environment*, 31, 2915–2931, doi:10.1016/S1352-2310(97)00126-X, <http://linkinghub.elsevier.com/retrieve/pii/S135223109700126X>, 1997.
- 1150 Wilson, K., Goldstein, A. H., Falge, E., Aubinet, M., Baldocchi, D. D., Berbigier, P., Bernhofer, C., Ceulemans, R., Dolman, H., Field, C., Grelle, A., Ibrom, A., Law, B., Kowalski, A., Meyers, T., Moncrieff, J. B., Monson, R. K., Oechel, W., Tenhunen, J., Valentini, R., and Verma, S.: Energy balance closure at FLUXNET sites, *Agricultural and Forest Meteorology*, 113, 223–243, doi:10.1016/S0168-1923(02)00109-0, <http://linkinghub.elsevier.com/retrieve/pii/S0168192302001090>, 2002.
- 1155 Wohlfahrt, G. and Cernusca, A.: Momentum transfer by a mountain meadow canopy: a simulation analysis based on Massman's (1997) model, *Boundary-Layer Meteorology*, 103, 391–407, 2002.
- Wolfe, G. M. and Thornton, J. A.: The Chemistry of Atmosphere-Forest Exchange (CAFE) Model – Part 1: Model description and characterization, *Atmospheric Chemistry and Physics*, 11, 77–101, doi:10.5194/acp-11-77-2011, <http://www.atmos-chem-phys.net/11/77/2011/http://www.atmos-chem-phys-discuss.net/10/21721/2010/>, 2010.
- 1160 Yamazaki, T., Kondo, J., and Watanabe, T.: A heat-balance model with a canopy of one or two layers and its application to field experiments, *Journal of Applied Meteorology*, 31, 86–103, 1992.

- 1165 Zhao, W. and Qualls, R. J.: A multiple-layer canopy scattering model to simulate shortwave radiation distribution within a homogeneous plant canopy, *Water Resources Research*, 41, 1–16, doi:10.1029/2005WR004016, <http://doi.wiley.com/10.1029/2005WR004016>, 2005.
- Zhao, W. and Qualls, R. J.: Modeling of long-wave and net radiation energy distribution within a homogeneous plant canopy via multiple scattering processes, *Water Resources Research*, 42, 1–13, doi:10.1029/2005WR004581, <http://doi.wiley.com/10.1029/2005WR004581>, 2006.

List of Figures

1170	1	Resistance analogue for a multilayer canopy approximation of n levels, to which the energy balance applies at each level. Refer to Table 1 for the interpretation of the symbols.	39
	2	Imposed Simulated Leaf Area Density Profile for corresponding to the forest canopy at Tumba Tower the Tumarumba site used in this study.	40
1175	3	Correlation of observed upwelling longwave radiation (derived from the measured above-canopy temperature) and the upwelling longwave radiation that is simulated by the model ORCHIDEE-CAN. Nighttime data (corresponding to a downwelling shortwave radiation of $<10W/m^2 < 10 Wm^{-2}$) are plotted in black, and daytime data are plotted in orange.	41
1180	4	Daily mean for measured (circles) and modelled (triangles) over a year-long run for (a) sensible heat flux; (b) difference between measured and modelled sensible heat flux; (c) latent heat flux; and (d) difference between measured and modelled latent heat flux. One in every 5 data points is shown, for clarity. Thick lines show the respective 20 day rolling moving average respectively for each dataset. Graphs (b) and (d) also show the overall mean of individual data points.	42
1185	5	Hourly means for measured (circles) and modelled (triangles) for (a) measured and modelled sensible heat flux; (b) difference between measured and modelled sensible heat flux, as calculated over a two the period of 2006 and 2007. 2006 . One in every 10th day is plotted for clarity; (c) and (d): as above for latent heat flux; (e) and (f): as above for net radiation. Continuous lines show the overall mean.	43
1190	6	<u>Short term simulated and observed energy fluxes:</u> (a) measured and modelled sensible heat fluxes at a height of 50m; (b) as (a) for latent heat flux; (c) measured and modelled sensible heat flux at 2m above the ground; (d) modelled latent heat flux at 2m above the ground (measurements not available); (e) difference in measured and modelled sensible and latent heat flux at a height of 50m	44
1195	7	Model run with an eddy coefficient forcing factor of unity. Plots show the seven day (6th November Vertical within canopy temperature profiles for four six-hour periods corresponding to 12th November 2006) mean the same time period as in Figure 6. Mean modelled temperature gradients profiles (bold in blue) within the canopy against the measured temperature gradients profiles (bold in red) for the time periods: (a) 0h00-6h00; (b) 6h00-12h00; (c) 12h00-18h00 and (d) 18h00-0h00, both expressed as a difference from the temperature at the top of canopy. Also shown are the measured and modelled data for each individual day, as dotted lines in the corresponding colour.	45
1200	8	Model run with smaller eddy coefficient factor <u>Comparison of 0.6 model performance for a set-up with 10 canopy layers (daytime out of 30 total profile levels) and 0.2, 5 canopy layers (nighttime of 15 total profile levels) within the, 2 canopy . Plots show the seven day levels (6th November to 12th November 2006 of 8 total profile levels) mean modelled temperature gradients (bold in blue) within the and 1 canopy against the measured temperature gradients levels (bold in red of 5 total profile levels), expressed as an hourly average for the time periods: a year-long run (a) 0h00-6h00 Root mean square difference between the different model runs for sensible heat flux; (b) 6h00-12h00; as (ea) 12h00-18h00 and for latent heat flux</u>	46
1210			

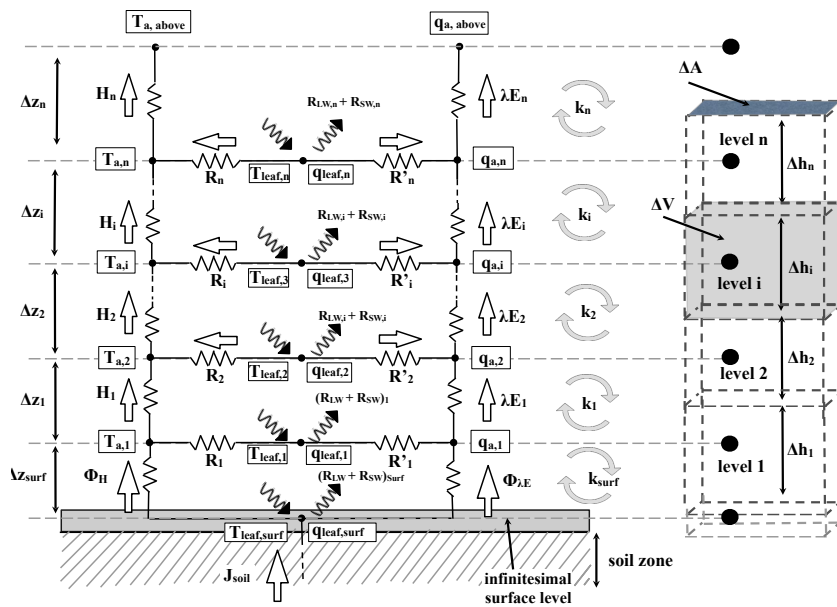


Figure 1. Resistance analogue for a multilayer canopy approximation of n levels, to which the energy balance applies at each level. Refer to Table 1 for the interpretation of the symbols.

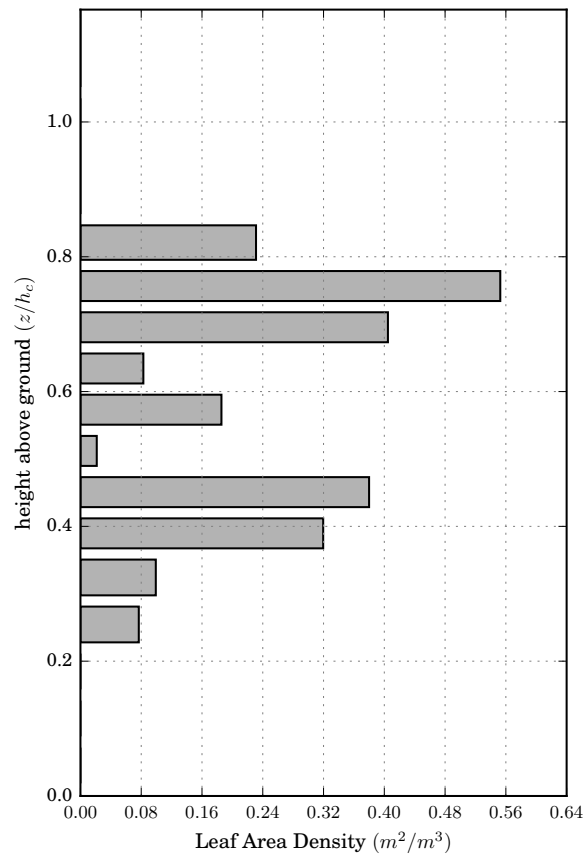


Figure 2. Imposed Simulated Leaf Area Density Profile for corresponding to the forest canopy at Tumba Tower the Tumbarumba site used in this study.

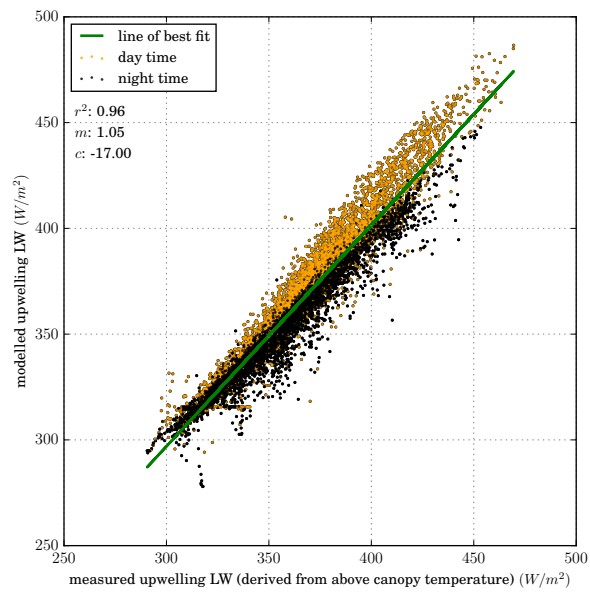


Figure 3. Correlation of observed upwelling longwave radiation (derived from the measured above-canopy temperature) and the upwelling longwave radiation that is simulated by the model ORCHIDEE-CAN. Nighttime data (corresponding to a downwelling shortwave radiation of $< 10 \text{ W/m}^2 < 10 \text{ W m}^{-2}$) are plotted in black, and daytime data are plotted in orange.

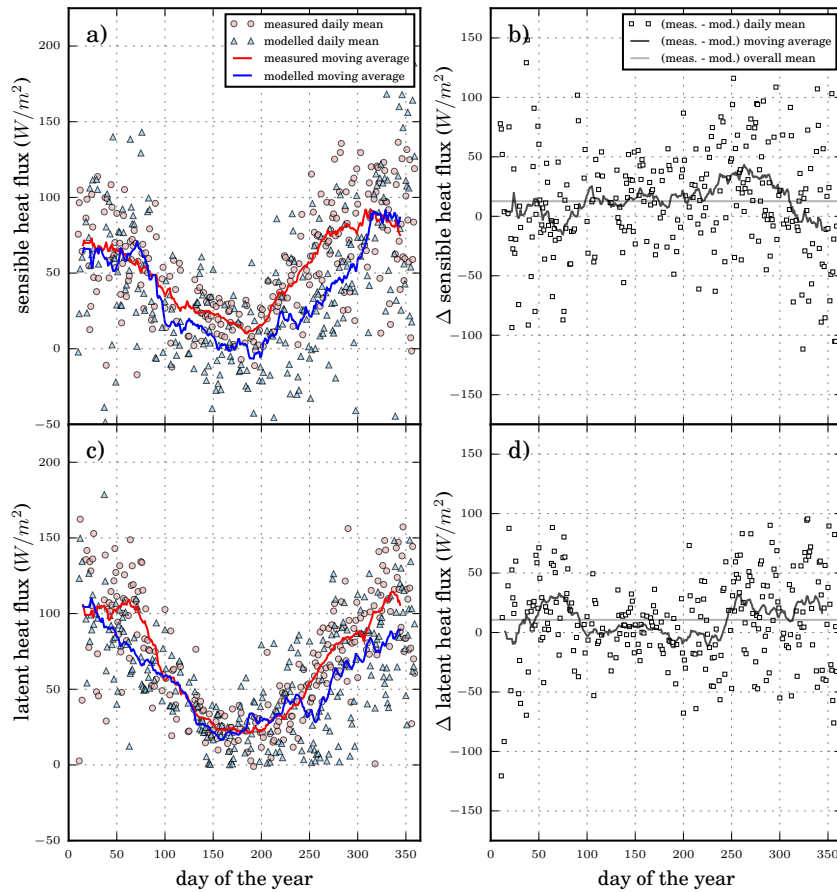


Figure 4. Daily mean for measured (circles) and modelled (triangles) over a year-long run for (a) sensible heat flux; (b) difference between measured and modelled sensible heat flux; (c) latent heat flux; and (d) difference between measured and modelled latent heat flux. One in every 5 data points is shown, for clarity. Thick lines show the respective 20 day [rolling moving](#) average respectively for each dataset. Graphs (b) and (d) also show the overall mean of individual data points.

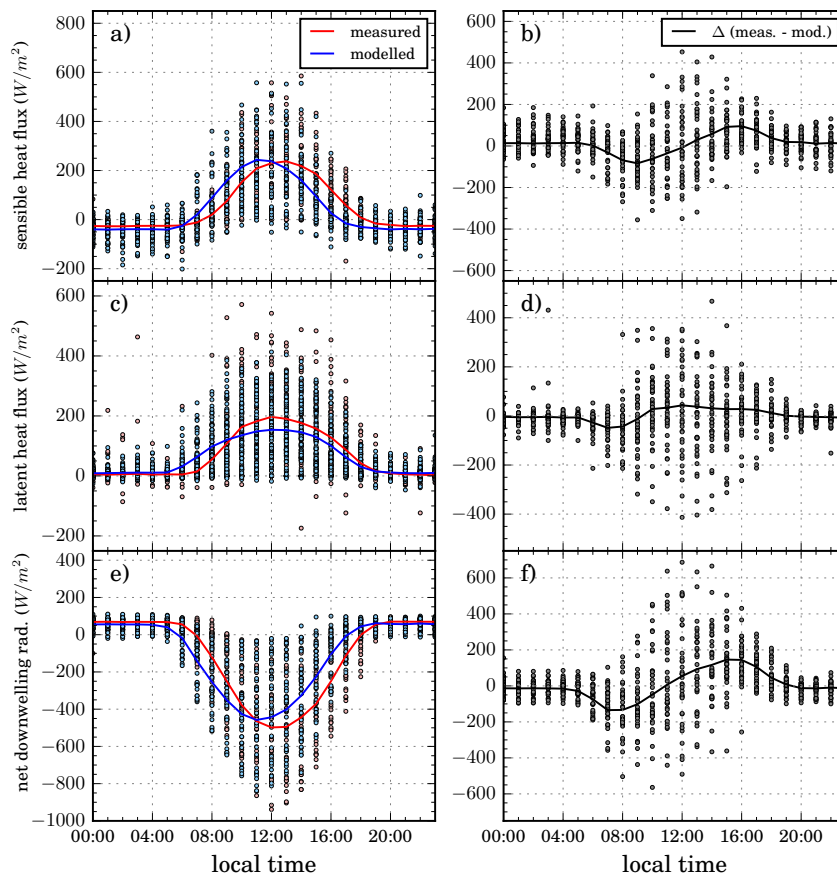


Figure 5. Hourly means for measured (circles) and modelled (triangles) for (a) ~~measured and modelled~~ sensible heat flux; (b) difference between measured and modelled sensible heat flux, as calculated over ~~a two~~ the period of ~~2006 and 2007-2006~~. One in every 10th day is plotted for clarity; (c) and (d): as above for latent heat flux; (e) and (f): as above for net radiation. Continuous lines show the overall mean.

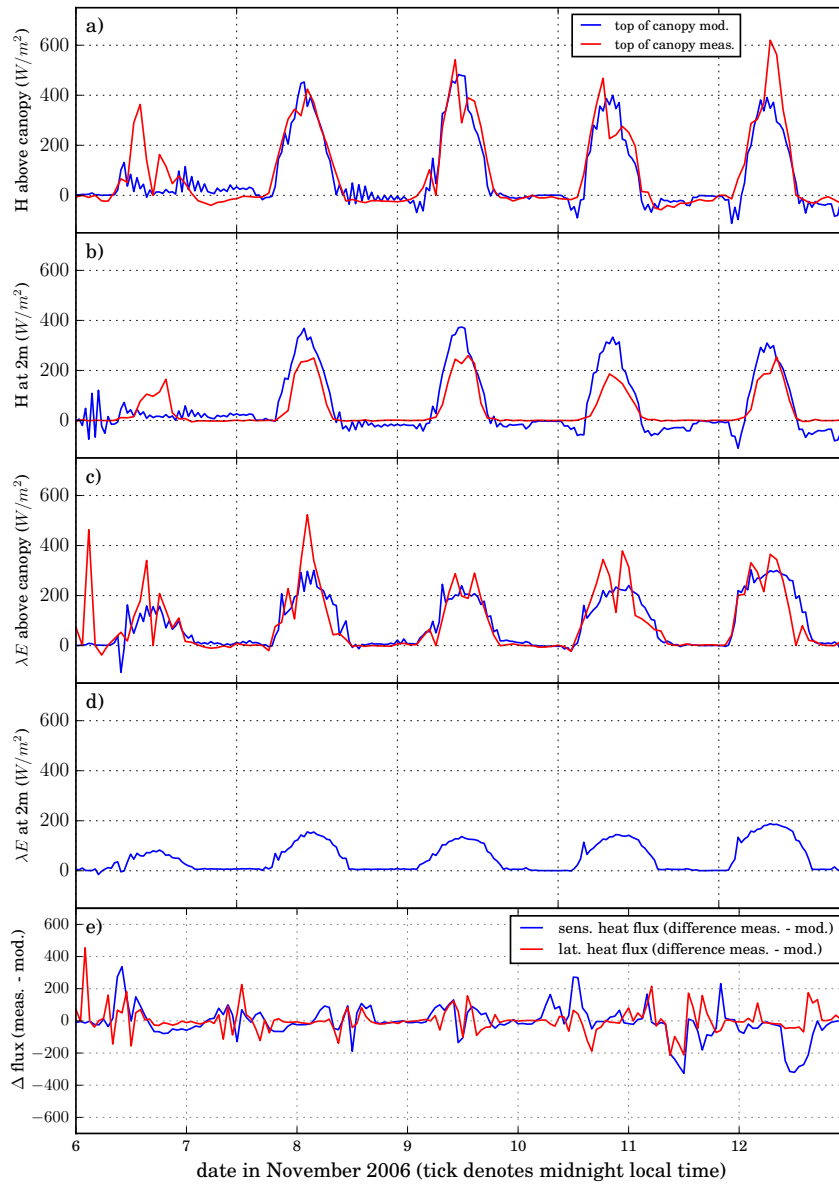


Figure 6. Short term simulated and observed energy fluxes: (a) ~~measured and modelled~~ sensible heat fluxes at a height of 50m; (b) as (a) for latent heat flux; (c) measured and modelled sensible heat flux at 2m above the ground; (d) modelled latent heat flux at 2m above the ground (measurements not available); (e) difference in measured and modelled sensible and latent heat flux at a height of 50m

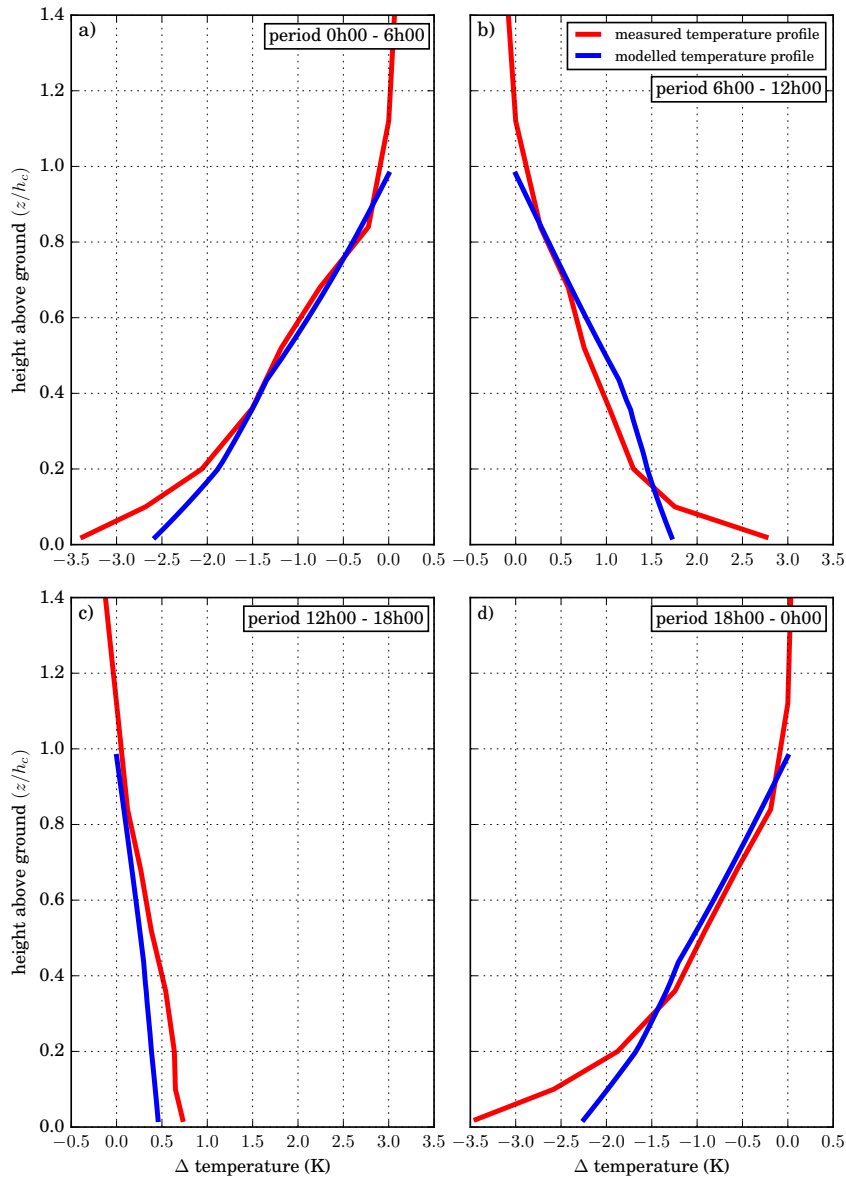


Figure 7. Model run with an eddy coefficient forcing factor of unity. Plots show the seven-day (6th November) vertical within canopy temperature profiles for four six-hour periods corresponding to 12th November 2006 mean the same time period as in Figure 6. Mean modelled temperature gradients profiles (bold in blue) within the canopy against the measured temperature gradients profiles (bold in red) for the time periods: (a) 0h00-6h00; (b) 6h00-12h00; (c) 12h00-18h00 and (d) 18h00-0h00, both expressed as a difference from the temperature at the top of canopy. Also shown are the measured and modelled data for each individual day, as dotted lines in the corresponding colour.

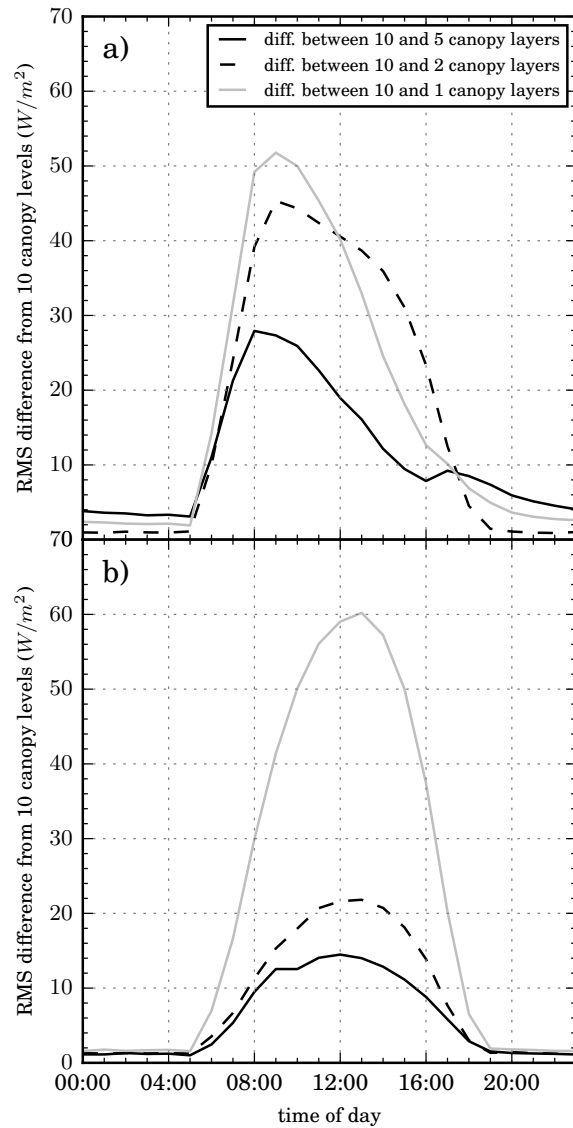
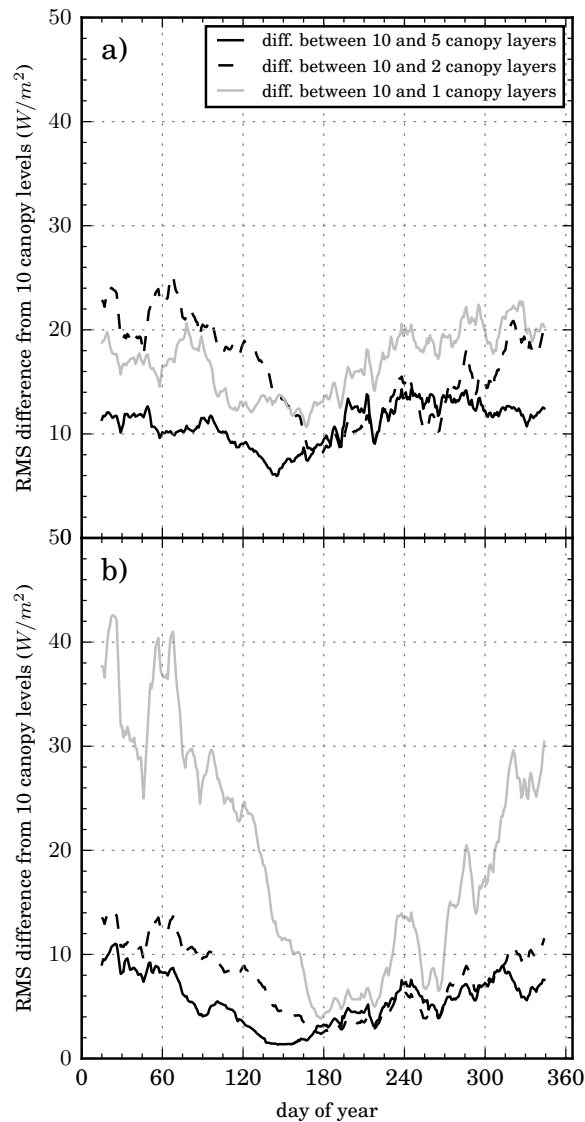


Figure 8. Model run with smaller eddy coefficient factor. Comparison of 0.6 model performance for a set-up with 10 canopy layers (daytime of 30 total profile levels) and 0.2, 5 canopy layers (nighttime of 15 total profile levels) within the 2 canopy. Plots show the seven-day levels (6th November to 12th November 2006 of 8 total profile levels) mean modelled temperature gradients (bold in blue) within the and 1 canopy against the measured temperature gradients levels (bold in red of 5 total profile levels), expressed as an hourly average for the time periods: a year-long run (a) 0h00-6h00 Root mean square difference between the different model runs for sensible heat flux; (b) 6h00-12h00; as (ea) 12h00-18h00 and for latent heat flux



(a) Root-mean-square difference between 50-level hourly average simulation of sensible heat flux and modelled 25-level, 10-level, 2-level and 1-level (plus the soil surface level) simulation of the same quantity; (b) as (a) for latent heat flux

a daily average (a) 20 day rolling-moving average of the root mean square difference of the daily mean ; between the 50-level simulation of sensible heat flux and modelled 25-level, 10-level, 2-level and 1-level (plus the soil surface level) simulation of the same quantity; (b) as (a) for latent heat flux

(a) Root-mean-square difference between 50-level hourly average simulation of sensible heat flux and modelled 25-level, 10-level, 2-level and 1-level (plus the soil surface level) simulation of the same quantity; (b) as (a) for latent heat flux

a daily average (a) 20 day rolling-moving average of the root mean square difference of the daily mean ; between the 50-level simulation of sensible heat flux and modelled 25-level, 10-level, 2-level and 1-level (plus the soil surface level) simulation of the same quantity; (b) as (a) for latent heat flux

Figure 9. As for Figure 8 for a set-up with 10 canopy layers (out of 30 total profile levels) 18h00-0h00, both expressed as a difference from the temperature at top 5 canopy layers (of 15 total profile levels), 2 canopy (Also shown are the measured levels (of 8 total profile levels) and modelled data 1 canopy levels (of 5 total profile levels), for each individual day a run over the course of a year, expressed as dotted-lines in the corresponding colour.

(a) Root-mean-square difference between 50-level hourly average simulation of sensible heat flux and modelled 25-level, 10-level, 2-level and 1-level (plus the soil surface level) simulation of the same quantity; (b) as (a) for latent heat flux

a daily average (a) 20 day rolling-moving average of the root mean square difference of the daily mean ; between

List of Tables

1215	1	Notation list Symbolic notation used throughout the manuscript (Latin)	49
	2	Input coefficients at the top layer of the model, where $A_{T,n}, B_{T,n}...$ etc are the respective coefficients at the top of the surface model and $A_{T,atmos}, B_{T,atmos}$ are the coefficients at the lowest level of the atmospheric model	51
	3	Tuning coefficients used in the model for simulation described in this work	52

Table 1. Notation list Symbolic notation used throughout the manuscript (Latin)

symbol	description
T^t, T^{t+1}	Temperature at the 'present' and 'next' timestep respectively (K) Components for substituted equation ii)
q^t, q^{t+1}	Specific humidity at the 'present' and 'next' timestep (kg/kg) Components for substituted equation i)
T_i^L	Leaf temperature at level 'i' (K) Specific heat capacity of air ($J/(kgK)$)
q_i^L	heat diffusivity of air (cm^2/s)
D_{H_2O}	heat diffusivity of water vapour (cm^2/s)
d_l	characteristic leaf length (m)
E_i, F_i, G_i	Components for substituted equation iii)
$G_{leaf}(\mu)$	Leaf orientation function
$H_i, \lambda E_i$	Sensible and latent heat flux at level i , respectively (W/m^2)
$H_{tot}, \lambda E_{tot}$	Total sensible heat and latent heat flux at canopy top, respectively (W/m^2)
$\mathcal{S}(\ell)$	effect of canopy structure on the passage of LW radiation
J_{soil}	Heat flux from the sub-soil (W/m^2)
k_i	Diffusivity coefficient for level i (m^2/s)
k_i^*	Modified diffusivity coefficient for level i (m^2/s)
k_{surf}	Diffusivity coefficient for the surface level (m^2/s)
l_i	cumulative Leaf Area Index, working up to level i (m^2/m^2)
Nu	Nusselt number (-)
Pr	Prandtl number (-)
$R_{b,i}, R'_{b,i}$	Boundary layer resistance at level i for heat and water vapour, respectively (s/m)
$R_{s,i}$	Stomatal resistance at level i (s/m)
R_i, R'_i	Total flux resistances at level i for sensible and latent heat flux, respectively (s/m)
$R_{LW,i}, R_{SW,i}$	Long-wave and short wave radiation received by level i , respectively (W/m^2)
R_{nf}	Lagrangian near field correction factor (-)
Re	Reynold's number (-)
q_i^a	Atmospheric specific humidity at level i (kg/kg)
$q_{leaf,i}$	Leaf specific humidity at level 'i' (kg/kg) (kg/kg)
$q_{sat}^{T_{leaf}}$	Saturated specific humidity of leaf at level at i (kg/kg)
q^t	Specific humidity (kg/kg)
Sh	Sherwood number (-)
T_i^a	Atmospheric temperature at level 'i' (K) (K)
q_i^a, T_L	Atmospheric specific humidity at level 'i' (kg/kg) Lagrangian timescale (s)
$\Delta T_{leaf,i}$	Interval between Leaf temperature at level i (K)
T^t, T^{t+1}	Temperature at the 'present' and 'next' timestep (s) respectively (K)

Table 1 (continued). Symbolic notation used throughout the manuscript (Greek)

c

A_{q,i}, B_{q,i}, C_{q,i}, D_{q,i} Components for substituted equation ii) *E_i, F_i, G_i* Components for substituted equation iii) *θ₀* Heat capacity of the infini

Table 2. Input coefficients at the top layer of the model, where $A_{T,n}, B_{T,n} \dots$ etc are the respective coefficients at the top of the surface model and $A_{T,atmos}, B_{T,atmos}$ are the coefficients at the lowest level of the atmospheric model

stand-alone model	coupled model
$A_{T,n} = 0$	$A_{T,n} = A_{T,atmos}$
$B_{T,n} = B_{T,input}$	$B_{T,n} = B_{T,atmos}$
$C_{T,n} = 0$	$C_{T,n} = 0$
$D_{T,n} = 0$	$D_{T,n} = 0$
$A_{q,n} = 0$	$A_{q,n} = A_{q,atmos}$
$B_{q,n} = B_{q,input}$	$B_{q,n} = B_{q,atmos}$
$C_{q,n} = 0$	$C_{q,n} = 0$
$D_{q,n} = 0$	$D_{q,n} = 0$

Table 3. Tuning coefficients used in the model for simulation described in this work

symbol (as here)	description	code ref.	initial value
$R_{b, fac}$ SUBSCRIPTNBfac	tuning coeff. for $R_{b,i}$ 1.0	br 0.857	-
$R_{g, fac}$ SUBSCRIPTNBfac	tuning coeff. for R_g 1.0	sr 2.426	-
number of levels	number of levels	nlvls	50-30
$R(\tau)R_{rel}$	eddy diff. tuning coef.	k_eddy_fac	1.0
m_{veg}	leaf mass	(leaf_tks*-rho_veg)	0.21 kg/m ²
$\Omega G_{leaf}(\mu)$ SUBSCRIPTNBgap-w	canopy gap fraction leaf orientation coeff. 1.0	canopybigk 0.4-0.75	Chen et al. (2005)-Gu et al. (1999)
$\rho_{albedo} a_3, a_4, a_5$	albedo coefficients for C_{Dell}	rhoSUBSCRIPTNBalbedo-a_3	0.2-0.452
K_{sw} SUBSCRIPTNBsw	SW extinction coefficient 0.5-	bigk a_4 0.4 a_5	1.876 Martens et al. (1993)-0.065